LAMP-5 is an essential inflammatory-signaling regulator and novel immunotherapy target for Mixed Lineage Leukemia-Rearranged acute leukemia

Gabriel Gracia-Maldonado, Jason Clark, Matthew Burwinkel, Brenay Greenslade, Mark Wunderlich, Nathan Salomonis, Dario Leone, Evelina Gatti, Philippe Pierre, Ashish Kumar, et al.

LAMP-5 is an essential inflammatory-signaling regulator and novel immunotherapy target in MLL-r leukemia

Gabriel Gracia-Maldonado[1, 2, 3], Jason Clark[2, 3], Matthew Burwinkel[3,5], Mark Wunderlich[2,5], Dario Leone[4], Philippe Pierre[4], Evelina Gatti[4], Lynn H. Lee[2, 7], Ashish R. Kumar[2, 3, 6]

Affiliations

[1]Pathobiology and Molecular Medicine Graduate Program, University of Cincinnati School of Medicine, Cincinnati, OH, 45267, USA.

[2]Cancer and Blood Diseases Institute, Cincinnati Children's Hospital Medical Center, Cincinnati, OH, 45229, USA

[3]Division of Bone Marrow Transplantation and Immune Deficiency, Cincinnati, Children's Hospital Medical Center, Cincinnati, OH, 45229, USA

[4]Aix Marseille Université, CNRS, INSERM, CIML, Marseille, France.

[5]Division of Experimental Hematology and Cancer Biology, Cincinnati, Children's Hospital Medical Center, Cincinnati, OH, 45229, USA

[6]Department of Pediatrics, University of Cincinnati School of Medicine, Cincinnati, OH, 45229, USA.

[7]Division of Oncology, Cincinnati Children's Hospital Medical Center, Cincinnati, OH, 45229, USA.

Running Title: The LAMP5 as a essential target of MLL-r leukemias

Keywords: Leukemia; MLL; LAMP5; innate Immunity

Conflict of Interest: The authors have declared that no conflict of interest exists.

Corresponding Author:
Ashish R. Kumar
Cincinnati Children's Hospital Medical Center
3333 Burnet Avenue, MLC 11027
Cincinnati, OH 45229
Phone#: (513) 803-2994
Email: Ashish.Kumar@cchmc.org

Abstract:

Although great advances have been made in understanding the pathobiology of MLL-rearranged (MLL-r) leukemias, effective therapies for this leukemia have remained limited, and clinical outcomes remain bleak. To identify novel targets for immunotherapy treatments, we compiled a lineage-independent MLL-r leukemia gene signature using publicly available data sets. Data from large leukemia repositories were filtered through the In-silico Human Surfaceome, providing a list of highly predicted cell surface proteins over-expressed in MLL-r leukemias. *LAMP5*, a lysosomal associated membrane protein, is expressed highly and specifically in MLL-r leukemia. We found that *LAMP5* is a direct target of the oncogenic MLL-fusion protein (MLL-FP). *LAMP5* depletion significantly inhibited leukemia cell growth *in vitro* and *in vivo*. Functional studies showed that LAMP-5 is a novel modulator of innate-immune pathways in MLL-r leukemias. Downregulation of *LAMP5* led to inhibition of NF-kB signaling and increased activation of type-1 interferon (IFN-1) signaling downstream of TLR/IL1R activation. These effects were attributable to the critical role of LAMP5 in transferring the signal flux from Interferon Signaling Endosomes (IRF-SE) to Pro-Inflammatory Signaling Endosome (PI-SE). Depletion of Interferon Response Factor 7 (IRF7) was able to partially rescue the cell growth inhibition upon *LAMP5* downregulation. Lastly, LAMP-5 was readily detected on the surface of MLL-r leukemia cells. Targeting surface LAMP-5 using an antibody drug conjugate lead to significant cell viability decrease specifically on MLL-r leukemias. Overall, based on our results and the limited expression throughout human tissues, we postulate that LAMP-5 could potentially serve as an immunotherapeutic target with a wide therapeutic window to treat MLL-r leukemias.

Introduction

Translocations in the Mixed Lineage Leukemia (*MLL*) gene account for 10% of all human leukemias and are associated with pediatric, adult, and therapy-related cases(1–3). In infants, around 80% of acute lymphoid leukemia (ALL) and 35%-50% of acute myeloid leukemia (AML) cases carry a translocation in the *MLL* gene (4–6). However, despite improvements in conventional chemotherapies treatments for leukemia, patients with MLL-rearranged leukemia (MLL-r) have poor response to treatment and poor prognosis (7, 8). Immunotherapy strategies have proven effective in multiple blood cancers, mainly targeting lineage specific proteins like CD19 (blinatumomab, tisagenlecleucel) and CD33 (gemtuzumab), abundantly expressed in Acute Lymphoid Leukemia (ALL) and Acute Myeloid Leukemia (AML) patients respectively(9). However, mounting evidence in recent clinical trials and case reports have shown that patients with MLL-rearrangements frequently relapse after treatment with CD19 immunotherapies, arising as AML or Mixed Phenotype Acute Leukemia (MPAL) (10–18). The exact mechanism of linage switch remains unclear, although several possible mechanisms have been proposed(11, 15, 18–22).

One approach to overcome this immune escape is to develop MLL-r specific immunotherapies targeting cell surface proteins essential for the survival of MLL-r leukemias. Gene-expression profiling based on underlying cytogenetic mutations is one way to identify proteins that are over-expressed and thus might be essential for the propagation of the specific leukemia(30–32). Both AMLs and ALLs with MLL-rearrangements share a common gene signature that is distinct from that of MLL-Germline (MLL-Germ) leukemias(33–35). Most of the well studied and validated MLL-r

gene targets however are DNA binding proteins like the HOXA gene cluster and its co-factor MEIS1(36–43), which are not suitable targets for immunotherapy.

Advances in labeling and mass spectrometry have provided new strategies to more accurately identify cell surface proteins in cancer(23). However, the focus has been on finding suitable targets for acute leukemias without distinguinshing between underlying cytogenetic mutations(24–27). The recently published in-silico human surfaceome provides a highly accurate surface protein dataset based on the experimental evidence from 41 human tissues within the Cell Surface Protein Atlas. This tool allows for further characterization of proteins-of-interest, specifically surface-expression (28, 29). In several of the published gene-expression studies, we found *LAMP5* significantly and specifically over-expressed in MLL-r leukemias(34, 35, 44–46). LAMP-5 is a member of the Lysosome-Associated Membrane Protein (LAMP) family. In contrast to other LAMPs, which show widespread expression, *LAMP5* expression in mice is confined to several regions of the postnatal brain. In neurons, the protein was found to recycle between the plasma membrane and a non-classical endosomal vesicle (47–49). In humans, aside from its conserved expression in the brain, LAMP5 is specifically expressed in plasmacytoid dendritic cells (pDCs)(50, 51). Upon activation of pDCs, LAMP-5 aids in the transport of Toll-Like Receptor 9 (TLR9) from early endosomal to lysosomal signaling vesicles, thereby regulating type 1 Interferon (IFN-1) and pro-inflammatory signaling respectively, downstream of TLR9 activation (52). Importantly, results of in silico modeling predict LAMP-5 as a cell-surface protein(29). In this report, we demonstrate *LAMP5* as being highly expressed and essential for MLL-r leukemias through the regulation of innate immune signaling, and describe its potential as a target for MLL-r specific immunotherapy.

Results

LAMP5 is highly expressed in MLL-r leukemias and is a direct target of the MLL-FP

To determine genes that are highly expressed in AML and ALL with MLL-rearragements, we compared recently published RNA-seq studies which identified differentially expressed genes between MLL-rearranged and MLL-germline leukemias in both AML and B-ALL samples(46, 53)(**Figure 1A).** Twenty seven genes were commonly over-expressed in MLL-r ALL and AML (**Supplemental table 1**). Using the In-silico Human Surfaceome tool (http://wlab.ethz.ch/surfaceome/) 5 of these 27 were predicted to be expressed on the cell surface(29) (**Supplemental table 1**). Of the 5 predicted proteins, Lysosomal Associated Membrane Protein 5 (LAMP-5) stood out for being present in multiple previous MLL-r leukemia gene expression studies(34, 35, 44, 45, 54) **(Supplemental Figure 1A-B)**. We further validated the specificity of *LAMP5* expression in MLL-r leukemias by analysing the 1,109 pediatric leukemia patient samples from the St.Jude PeCan Portal which again revealed *LAMP5* as significantly overexpressed in both AMLs and ALLs with MLL-rearragements **(Figure 1B)**(30, 31)**.** To determine if *LAMP5* expression could discriminate between MLL-r leukemia and MLL-Germ leukemia patients, we performed a Receiving Operating Curve (ROC) analysis. *LAMP5* achieved a statistically significant AUC (area under the curve) score in both the Microarray Innovations in Leukaemia (MILE) (GSE13159) and the St. Jude PeCan datasets, with high sensitivity and specificity at the optimal cutoff points (**Figure 1C**). Further, a Kaplan-Meier survival analysis of B-ALL and AML patients correlated higher expression of *LAMP5* with poor survival (**Supplemental Figure 2**). High levels of *LAMP5* mRNA expression **(Figure 1D**) and protein (**Figure 1E**) were also observed in human myeloid

and lymphoid MLL-r leukemia cell lines (MOLM-13, MV4;11, THP-1, and RS4;11) as compared to MLL-Germ leukemia cell lines (HL-60, Kasumi-1, K562, REH and RCH-ACV) and normal human CD34-enriched cord blood cells (CB-CD34$^+$ cells).

Translocations of the *MLL* locus generate MLL-fusion proteins (MLL-FP) which activate transcription of downstream target genes(55–58). To determine if *LAMP5* expression was dependent on the MLL-FP, we transformed CB-CD34$^+$ cells with a retrovirus carrying a tetracycline-repressible MLL-AF9 construct. Treatment of transformed cells with Doxycycline led to a simultaneous reduction in the levels of both *MLL-AF9* and *LAMP5*. (**Figure 1F**). To determine if the MLL-FP directly activates the *LAMP5* gene locus, we interrogated previously published MLL-AF4 chromatin immunoprecipitation sequencing (ChIP-seq) datasets derived from the RS4;11 cell line, and those from CD34$^+$ cells transformed with FLAG-MLL-AF4. Coincident ChIP-seq signals of MLL N-terminus and AF4 C-terminus showed MLL-FP binding at the promotor region of *LAMP5*(55, 56, 58). Additionally, there was accompanying significant enrichment of H3K4me3 and H3K79me2 at the gene locus, confirming that *LAMP5* is a direct target of the MLL-FP complex (**Figure 1G**). In mice, *Lamp5* is not expressed in blood, as it is in human (Supplemental Figure 3A-B). Furthermore, we did not detect upregulation of *Lamp5* in mouse models of MLL-AF9, E2A-HLF and AML1-ETO leukemia, hence we focused our studies exclusively on human cells **(Supplemental Figure 3C)**.

LAMP-5 is required for *in vitro* and *in vivo* leukemia cell survival

The ideal immunotherapy target should be essential for the survival of MLL-r leukemias. To test the functional role of LAMP-5 in MLL-r leukemia, we transduced both MLL-r leukemia (MOLM-13, MV4;11, RS4;11, THP-1) and MLL-Germ leukemia cells (Kasumi-1

and REH) with lentiviral shRNA vectors targeting *LAMP5*. We obtained efficient knockdown of *LAMP5* with 2 independent hairpins as compared to non-targeting control (NT) **(Supplemental Figure 4A)**. Upon *LAMP5* depletion, we observed a significant reduction of cell growth in MLL-r leukemia cell lines (**Figure 2A**), while no effect was seen in MLL-Germ/LAMP-5-negative leukemia cell lines, Kasumi-1 and REH **(Figure 2B).** Additionally, *LAMP5* knockdown led to a significant decrease in colony forming units (CFU) in the MLL-r leukemia cell lines **(Figure 2C)** suggesting an effect on the clonogenicity of these cells. Furthermore, *LAMP5* knockdown led to apoptosis in MLL-r leukemia cells, as evident by a significant increase in Annexin V and 7-AAD double positive staining **(Figure 2D;Supplemental Figure 4B)**. We next sought to determine the role of LAMP-5 in leukemia propagation *in vivo*. MV4;11 cells were transduced with shRNAs targeting either *LAMP5* or a NT control followed by transplantation into immunocompromised NOD-*Rag1*^{null} *IL2rγ*^{null} (NRG) mice (8 mice per shRNA group). Viral transduction was confirmed by flow cytometry for Venus expression. Four weeks after transplantation, mice developed signs of leukemia and were sacrificed. In the bone marrow, both groups showed similar human cell engraftment based on human CD45 expression. On the other hand, the transduced Venus^{+} fraction was significantly reduced in shLAMP5-2 compared to shNT mice. (**Figure 2E, left panels**). We repeated this experiment using cells from a patient with MLL-r (MLL-AF10) leukemia. We again observed significant reduction in the proportion of Venus^{+} cells with *LAMP5* knockdown compared to NT control **(Figure 2E, right panels)**. Overall, these data underscore a critical role for LAMP-5 in the growth of MLL-r leukemia cells.

LAMP-5 is required for activation of TLR/IL1R signaling in leukemia

Acute leukemias exhibiting constitutive activation of innate immune signaling pathways have been characterized as having a pro-inflammatory profile which is required for their survival(59, 60). These physiologic cellular systems involve TLR/IL1R signaling and culminate in the release of pro-inflammatory cytokines via NF-kB and/or of type I interferons (IFN-1)(61). Recent studies reveal heightened activation of NF-kB signaling in MLL-r leukemia compared to other leukemias(62). Furthermore, MLL-r leukemias have been shown to require the TLR/IL1R signaling pathway to survive, through degradation of the wild-type MLL protein, allowing the MLL-FP to bind to its target genes without restriction(63). Recently, Combes et al. showed that LAMP-5 plays an important role in controlling the subcellular location of TLR9 after activation in human pDC. Upon activation of TLR9, LAMP-5 shuttles TLR9 from the VAMP3^{+}-Interferon Response Factor signaling endosome (IRF-SE), to the LAMP-1^{+}-pro-inflammatory-signaling endosome (PI-SE). This transition of TLR localization in turn acts as a negative regulator of IFN-1 signaling (52). Based on the known role of LAMP-5 in TLR9 localization in pDCs, we first examined the localization of intracellular LAMP-5 in MOLM-13 cells. We performed co-staining of MOLM-13 cells with antibodies against LAMP-5, LAMP-1 and Myeloid Differentiation Primary Response 88 (MYD88), a scaffold protein that is required for TLR and IL1R signaling (63–65). Confocal microscopy showed that in MLL-r leukemia cells, LAMP-5 localized to LAMP-1^{+} vesicles. As suspected, we found MYD88 accumulating highly in the periphery of LAMP-1^{+} vesicles in MLL-r leukemia, suggestive of TLR/IL1R activation **(Figure 3A)**. Conversely, in the LAMP-5-negative MLL-Germ leukemia cells (Kasumi-1),

MYD88 does not co-localize with LAMP-1$^+$ vesicles. However, overexpression of LAMP-5 in this cell line led to relocation of MYD88 around LAMP-1$^+$ vesicles **(Figure 3B)**.

We subsequently hypothesized that LAMP5 loss may dampen TLR/IL1R signaling in MLL-r leukemias. We thus analyzed known effector proteins downstream of TLR/IL1R activation by western blot. Upon *LAMP5* knockdown, we observed a reduction in phosphorylated NF-kB, p38, and JNK, key players in the signal transduction downstream of TLR/IL1R **(Figure 3C)**. To further determine the impact of *LAMP5* depletion on activation of NF-kB downstream of TLR activation, we measured NF-kB activity using the MLL-r cell line THP-1Blue-NF-kB, which contains an NF-κB inducible Secreted Embryonic Alkaline Phosphatase (SEAP) reporter. Robust activation of NF-kB was evident in control cells upon incubation with PAM3CSK4 (TLR2 agonist) or LPS (TLR4 agonist). Knockdown of LAMP-5 led to near-complete blockade of this activation, suggesting that TLR-induced NF-kB signaling is disrupted upon LAMP-5 depletion **(Figure 3D)**. Correspondingly, in the LAMP-5 negative cell line Kasumi-1, overexpression of *LAMP5* led to increased phosphorylation of p38, JNK and NF-kB along with increased cell growth**(Figure 3E-F).**

Previous studies have shown that NF-kB plays a critical role in MLL-r leukemias (62). We thus hypothesized that NF-kB activation would rescue the cell growth defect seen by LAMP5 depletion. We induced persistent activation of NF-kB in leukemia cells by overexpressing a constitutively active version of Inhibitor Of Nuclear Factor Kappa B Kinase Subunit Beta (IKBKB-EE) in these cells. The IKBKB-EE is a variant of IKBKB that contains mutations at Ser^{177} and Ser^{188} leading to constant degradation of IκB-α kinase (66, 67). Despite sustained NF-kB activation, knockdown of LAMP-5 in MOLM-13 and

RS4;11 cells still led to growth inhibition, suggesting that loss of NF-kB is not the only signaling event being affected by LAMP5 depletion **(Supplemental Figure 5A-B)**. A potential mechanism underlying this essentially was proposed by Wang et al, where they suggested that loss of LAMP5 in MLL-r leukemia led to degradation of the MLL-FP due to increased autophagy(68). However, in our experiments we did not observe any change in the levels of the MLL-FP in THP1 and MOLM-13 cells upon LAMP-5 depletion (**Supplemental Figure 4C**). Overall, these results underscore a critical role for LAMP-5 in the activation of TLR/IL1R signaling in MLL-r leukemia, while also indicating the presence of additional attributes that are also essential.

LAMP-5 is a negative regulator of IFN-1 signaling in MLL-r leukemias

Since activation of NF-kB was not sufficient to rescue the cell growth inhibition seen upon LAMP-5 depletion, we next sought to understand the mechanistic significance of the inflammatory-signal-regulation function of LAMP-5 in MLL-r leukemia. In pDCs, the carboxy-terminal YKHM domain of LAMP-5 was found to be required for normal localization of LAMP-5 and for transportation of TLR9 from the early endosome vesicle to the pro-inflammatory vesicle (47, 50, 52). We thus overexpressed wild-type LAMP-5 (LAMP-5-WT), a YKHM mutant (LAMP-5-Y276A), or control vector (EV) in MV4;11 and THP-1 cells, followed by selective knockdown of endogenous *LAMP5* using an shRNA targeting the 3'UTR region of *LAMP5*. Overexpression of LAMP-5-WT completely prevented the cell growth inhibition upon knockdown of endogenous *LAMP5*, validating *LAMP5* as the main target of the shRNA. In contrast, LAMP-5-Y276A was unable to rescue the cell growth in both MV4;11 and THP-1 cell lines **(Figure 5A)**. In pDCs, *LAMP5* knockdown or overexpression of LAMP-5-Y276A induced IFN-1 activation upon TLR9-

stimulation, due to retention of TLR9 in the IRF-SE. To determine the effect of LAMP-5 on IFN-1 signaling in MLL-r leukemia, we turned to THP-1-ISG-SEAP cells that contain an Interferon Stimulated Gene (ISG) inducible-SEAP reporter. Upon TLR activation by PAM3CSK4, IFN-1 signaling activation was evident only in the LAMP-5-depleted cells but not in the control LAMP-5 depleted condition **(Figure 5B)**. To ensure this effect was not limited to one cell line, we validated the increase in IFN-1 signaling in other MLL-r cell lines by demonstrable increased expression of Interferon Regulatory Factor 7 (*IRF7)*, one of the downstream effectors of TLR activation, Interferon Alpha 2 (*IFNA2)* and Signal transducer and activator of transcription 1 (*STAT1)* upon depletion of LAMP-5 (**Figure 5C)** (69). To assess the role of LAMP5-depletion mediated IFN-1 activation on cell growth, we performed knockdown of *IRF7* along with *LAMP5 in* MV4;11 cells**.** We found that loss of IRF7 alone had no significant effect on MLL-r leukemia cell growth but importantly, its depletion prevented the growth inhibition observed upon LAMP-5 knockdown **(Figures 5D and 5E) (Supplemental Figure 6A-B)**. Collectively, these results demonstrate that a critical function of LAMP-5 in MLL-r leukemias is to promote the transfer of TLR/IL1R from the IFN-1–activating signaling cascade to the pro-inflammatory signaling cascade. Depletion of LAMP-5 thus leads not only to loss of NF-kB activation but also to activation of IFN-1-signaling, the latter inducing cell-death.

Surface LAMP-5 can be detected and targeted with Antibody Drug Conjugate therapy

Previous studies have shown that all LAMP family members can localize to the plasma membrane (70–73). Furthermore, LAMP-5 was found to briefly localize in the plasma membrane of cortical neurons in mice, and is highly predicted to reach the cell membrane

based on the human surfaceome(29, 47). We thus sought to confirm if LAMP-5 was expressed on the surface of MLL-r leukemia cells. Using an antibody targeting the N-terminus of LAMP-5, we were able to detect LAMP-5 on the surface of MLL-r leukemia cell lines, while none was detected in the MLL-Germ leukemias (**Figure 5A-B**). To validate the specificity of the antibody, we overexpressed LAMP-5 or control empty vector (EV) in the LAMP-5-negative MLL-Germ leukemia cell line, Kasumi-1. We detected surface LAMP-5 only in the cells that express high levels of LAMP-5 **(Figure 5C)**. Using primary AML patient samples, we further validated that surface LAMP-5 can discriminate between MLL-r leukemia and MLL-Germ leukemias **(Figure 5D)**. As proof-of-concept for potential therapeutic use, we used a secondary antibody conjugated to the tubulin-toxin Mertansine, targeting the surface-LAMP-5 antibody. We observed that a 72-hour treatment with this antibody-sandwich comprised of the surface LAMP-5 antibody along with the secondary ADC antibody is sufficient to reduce cell viability in MLL-r leukemia cell lines MOLM-13, RS4;11 and THP-1, while no effect was seen in the LAMP-5-negative Kasumi-1 cell line **(Figure 5E)**. These results suggest that LAMP-5 could be exploited as a MLL-r specific biomarker and could potentially be used as a target for immunotherapy.

Discussion

Our findings identify *LAMP5* as a novel core gene in MLL-r leukemias, directly up-regulated by the MLL-FP. Additionally, we found that LAMP-5 is essential for MLL-r leukemia cell survival. Further, we found that one of the critical functions of LAMP-5 is to regulate innate-immune signaling in MLL-r leukemias, specifically directing the flux of activity away from IRF-SE towards the PI-SE, leading to constant activation of NF-kB.

Recent discoveries have highlighted how the specific subcellular location and timing of TLR activation affect signaling outcomes in normal immune cells(74). However, how these mechanisms function in leukemia is still poorly understood. Recently, Combes et al. showed that LAMP-5 is a negative regulator of IFN-1 signaling in pDCs by transporting activated TLR9 from the IRF-SE to the PI-SE. Although dispensable for pDCs cell survival, LAMP-5 depletion leads to unrestricted activation of IFN-1 signaling. Furthermore, aberrant expression of LAMP-5 can lead to diminished activation of pDCs in tumors and contribute to their immunomodulatory phenotype by decreasing the IFN-1 production capacity(52). Innate immune signaling and inflammation have been shown to play a crucial role in acute leukemias(59, 60). MLL-r leukemias rely on activation of NF-kB downstream of TLR/IL1R to maintain the MLL-FP gene signature and block cell differentiation(62, 63). Furthermore, it has been shown that treatment with IFN-β or activation of IFN-1 signaling is deleterious for MLL-r leukemias (75). In our study, we describe a novel role for LAMP-5 in maintaining NF-kB activation and blocking IFN-1 signaling downstream of TLR/IL1R activation in MLL-r leukemias. We show that LAMP-5 acts as a molecular switch to maintain TLR/IL1R signaling in the pro-inflammatory endosome leading to NF-kB activation, whereas LAMP-5 depletion leads to activation of IFN-1 signaling and cell death. This suggests that both LAMP-5-mediated induction of pro-inflammatory signaling and inhibition of IFN-1 signaling contribute to the pathogenesis of MLL-r leukemias. We confirmed that activated IFN-1 signaling upon LAMP-5 depletion induced cell death by depleting IRF7, which rescued cell growth and clonogenicity in LAMP5-depleted cells. This suggests that increased IFN-1 signaling is at least partly responsible for inducing cell death upon LAMP-5 depletion. Additionally, overexpression

of *LAMP5* in MLL-Germ leukemia leads to increased activation of NF-kB, p38 and JNK, and increased cell growth, which suggests that this signaling pathway might be contributing to the therapy-resistant phenotype of MLL-r leukemias.

LAMP-5 is part of the lysosomal associated membrane protein family, of which two main members LAMP-1 and LAMP-2 are expressed in the endo-lysosomal vesicles ubiquitously in all tissues (76). In contrast, LAMP-3 and CD68 (LAMP-4, microsialin) show a more restricted expression in human tissues (72, 77). Regardless of their prominent localization in the endo-lysosomal compartment of cells, all LAMP members have been shown to localize in the plasma membrane either at steady state or as a result of immune activation(70–73). In humans, *LAMP5* expression is generally restricted to the brain, ovaries and blood. In blood, *LAMP5* is exclusively expressed in nonactivated pDCs (50, 51). Interestingly, in non-activated pDCs, LAMP-5 is found in the ERGIC compartment and it requires the activation of TLR9 to leave the compartment and join the endo-lysosomal vesicles(50, 52). We found that the aberrant increased expression of LAMP-5 in MLL-r leukemia leads to its accumulation in the plasma membrane, as evidenced by a novel LAMP-5 antibody targeting the N-terminus of the protein. The detection of LAMP-5 on the surface of MLL leukemias provides the opportunity to potentially use it as a target for immunotherapy in this treatment-refractory malignancy. These results provide a rationale to develop immunotherapies targeting LAMP-5. Furthermore, LAMP5 is highly expressed in other cancers such as multiple myeloma (MM) and blastic plasmacytoid dendritic cell neoplasm (BPDCN)(78, 79). Therefore LAMP5 immunotherapies could benefit other blood diseases. Finally, total loss of Lamp5 in mice had no major effects on

health or lifespan with minor behavioral effects, suggesting that there could be a wide therapeutic window for LAMP-5-directed therapies in humans (48, 49).

Similar to our observations, Wang et al. recently showed that LAMP-5 is essential for the survival of MLL-r leukemias *in vitro* and *in vivo* using shRNA knockdown. However, they propose that LAMP-5 is a negative regulator of autophagy leading to MLL-FP stabilization. They show that LAMP-5 and ATG5 colocalize in MLL-r leukemia cells and that blockade of autophagy is sufficient to rescue the increased levels of apoptosis after LAMP-5 knockdown(68). We were unable to detect any significant change in the levels of the MLL-FP upon LAMP5 knockdown. Since TLR-mediated innate immune signaling can regulate autophagy, it is possible that the function of LAMP-5 in regulating autophagy as described by Wang et al is downstream of its impact on endosome-lysosome trafficking(80–84). On the other hand, it is also possible that these effects are not directly linked and that LAMP-5 might exert its growth-promoting effects in MLL-r leukemia by multiple mechanisms. It is notable however that the role of autophagy in leukemia is controversial(85). In murine MLL leukemia models, heterozygous loss of *Atg5* leads to increased leukemia cell proliferation *in vitro* and more aggressive leukemia *in vivo*, while homozygous loss is lethal to these cells(86). Additionally, while some studies suggest that Atg5-dependent autophagy may contribute to the development of MLL-AF9 driven leukemia but dispensable for propagation and chemosensitivity, others suggest that Atg5-dependent autophagy is dispensable altogether(87–89). Overall, our results show that LAMP-5 localizes both on the surface and in LAMP-1^{+} endosomes in leukemia, leading to constitutive activation of pro-inflammatory signaling, and dampening of interferon-signaling, and that it can be used as a target for immunotherapy.

Materials and Methods:

Cell lines and primary patient cells

Human leukemia cell lines were maintained in Iscove's modified Dulbecco medium (IMDM) or Roswell Park Memorial Institute (RPMI) 1640 medium supplemented with 10% fetal bovine serum (FBS), 1% penicillin and 1% streptomycin.

MLL-AF9 Tet-off human $CD34^+$ cells were a kind gift from Dr. James Mulloy, and were generated as follows: umbilical cord blood (UCB) was obtained from the Translational Trial Development and Support Laboratory of CCHMC. $CD34^+$ cells were isolated from UCB using the EasySep $CD34^+$ isolation kit (StemCell Technologies). $CD34^+$ cells were pre-stimulated in IMDM/20%FBS containing 100ng/mL SCF, TPO, Flt3-L, and IL-6 and 20ng/mL IL-3 for 2 days before transduction. Transduction was carried out using spinoculation onto Retronectin (Takara Bio) coated plates along with 4ug/mL polybrene. Cells were transduced with both the pSIN-TREtight-dsRED-MLL/AF9 lentivirus and the MSCV-GFP-IRES-tTA34 retrovirus. After transduction, cells were maintained in IMDM/20% FBS with 10ng/mL of each cytokine. A pure population of $dsRED^+GFP^+$ cells were selected over several weeks of culture.

Fully de-identified primary patient cells were obtained from the Cincinnati Children's Hospital Medical Center Biorepository. Patient identities have been protected. By the time the mice displayed signs of leukemia, the only human cells that remained in the mice were leukemic cells (MLL-rearrangement was confirmed with FISH).

Human $CD34^+$ cells and cells from patients with MLL-r AML were cultured in IMDM supplemented with 20% FBS and 10 ng/ml human cytokines including SCF, FLT3-Ligand,

Thrombopoietin, IL-3 and IL-6. Cell lines were periodically validated by STR genotyping through Genetica Cell Line Testing (LabCorp). Cells were tested and were negative for mycoplasma contamination. None of the cell lines utilized in this study are recognized by the ICLAC as being commonly misidentified.

Animal experiments

All animals used for this study were 6-12 weeks old. All animal experiments were carried out in accordance with the guidelines of the Institutional Animal Care and Use Committee (IACUC). For xenograft experiments with MV4;11 and MLL-r primary patient cells, immunocompromised NOD-*Rag1*^{null} *IL2rγ*^{null} (NRG) (Jackson Laboratories, stock no. 007799) recipient mice were conditioned with 30 mg/kg busulfan and transplanted with 2-7.5x10^5 cells 24 hours later. In xenograft experiments bone marrow samples were collected four weeks after transplantation as well as when signs of leukemia were present; aspirates were analyzed via flow cytometry for the presence of human CD45$^+$ cells and the presence of shRNA-transduced Venus$^+$ cells

Retroviral and lentiviral transductions

Retroviral and lentiviral supernatants were generated by transfection of HEK293T cells using the FuGENE 6 reagent (Promega) according to the manufacturer's recommendations.

The lentiviral shRNA pLKO.1-Puro plasmids TRCN0000129410 (shLAMP5-1), TRCN0000129378 (shLAMP5-2) and TRCN0000014861 (shIRF7) were purchased from Millipore Sigma. Human cells were incubated with a single dose of lentiviral supernatant overnight. Cells transduced with constructs granting puromycin resistance were selected

in 0.5-5 ug/ml of Puromycin for 72 hours. Cells transduced with constructs containing a fluorescent marker (Venus) were isolated on between days 4-5 after transduction by sorting using MoFlo XDP, FACSAria (BD Biosciences) or a SONY SH800S (Sony Biotechnology

The retroviral IKBKB-S177E-S181E (IKBKB-EE) plasmid was a gift from Anjana Rao (Addgene plasmid # 11105; http://n2t.net/addgene:11105; RRID:Addgene_11105). Flag-LAMP5-WT and Flag-LAMP5-Y276A plasmids were as described previously(47) FLAG-LAMP5-WT and FLAG-LAMP5-Y276A were cloned into the MSCV-IRES-Puro vector.

Flow cytometry

For apoptosis assays, cells were incubated with allophycocyanin (APC)-conjugated Annexin V (BD Bioscience) for 15 minutes at RT in 1X Annexin V Binding Buffer (BD Bioscience) followed by staining with 7-aminoactinomycin (7-AAD) (eBioscience). For surface LAMP-5 detection, cells were incubated with 3 µg anti-human LAMP-5 therapeutic antibody (TAB-0643CL, Creative Biolabs, NY, USA) overnight and then stained with anti-mouse IgG1-PE (eBioscience). Data were acquired on a FACS Canto I and results were analyzed using FlowJo Version 10 (FlowJo).

Colony-forming unit assays

Transduced human cells were sorted 4-5 days after transduction and were cultured in methylcellulose-containing media (StemCell Technologies, H4434). Colonies were scored 10-14 days after plating.

RT- and Quantitative RT-PCR

Total RNA was extracted from human Puromycin-selected or sorted Venus^{+} cells using the RNeasy Mini kit (Qiagen). RNA was reversed transcribed into cDNA using iScript Advanced cDNA Synthesis kit (Bio-Rad Laboratories). For Quantitative RT-PCR 5-10ng of cDNA was analyzed using iTaq Universal SYBR Green Supermix and iTaq Universal Probes Supermix (Bio-Rad) in a StepOnePlus Real-Time PCR machine (Applied Biosystems). Taqman probes were purchased from Applied BioSystems. Primers and probes used for Quantitative RT-PCR were: *LAMP5* (5'-TACGACTCCTCGGAGAAAACC-3' and 5'-TGACACTCATAGGACTTCCCAG-3') *IRF7* (5'-CCCACGCTATACCATCTACCT-3' and 5'-GATGTCGTCATAGAGGCTGTTG-3'), *LAMP5*(Hs00202136_m1), *STAT1* (Hs01013996_m1), *IFNA2* (Hs00265051_s1), *ACTIN* (Hs99999903-m1)

Western blotting

The primary antibodies used were anti-LAMP-5 (Thermo Fisher Scientific Cat# 14-9778-80, RRID:AB_2573029), anti-AF9 (Bethyl Cat# A300-597A, RRID:AB_495520), anti-MLL1 (Cell Signaling Technology Cat# 14689, RRID:AB_2688009), anti-phospho-JNK (Cell Signaling Technology Cat# 4668, RRID:AB_823588), Phospho-IKK (Cell Signaling Technology Cat# 2697, RRID:AB_2079382), Phospho-p38 MAPK (Cell Signaling Technology Cat# 4511, RRID:AB_2139682), Phospho-NF-kB p65 (Cell Signaling Technology Cat# 4025, RRID:AB_10827881), anti-Actin (Cell Signalling Technology, 13E5, RRID: AB_2223172), and anti- β-tubulin (Cell Signaling Technology, 9F3, RRID: AB_823664). Whole cell lysates were isolated using RIPA buffer (Sigma) and the amount of protein was determined using the BCA Protein Assay Kit (Thermo Scientific). 30 µg of

protein was separated by SDS-PAGE on a 4-20% gradient gel (Bio-Rad). After transfer to PVDF membranes, blots were blocked with Odyssey® Blocking Buffer TBS (LI-COR) for one hour and incubated with primary antibodies overnight. After washing, blots were incubated with appropriate secondary IRDye 680RD goat anti-mouse (LI-COR) and IRDye 800CW goat anti-rabbit (LI-COR) antibodies at a dilution of 1:10,000 for one hour. Images were obtained using the Odyssey CLx Infrared Imaging System (LI-COR).

ChIP-seq Analysis

ChIP-seq data were downloaded from the Gene Expression Omnibus using the listed accession numbers (GSE84116 for MLL-Af4 transformed CB $CD34^+$, GSE95511 for ML-2 data, GSE79899 for MV4;11 and THP-1 data, GSE38403 for RS4;11 data, and GSE38338 for SEM data) and visualized with the UCSC Genome Browser, assembly hg19. For consistency, data for RS4;11 and SEM were converted from their originally mapped hg18 to hg19 using the liftOver tool from the UCSC Genome Browser Utilities.

Cell Viability

MOLM-13, RS4;11, THP-1 and Kasumi-1 cells were plated at 10,000 cells per well in a 96-well plate. Cells were incubated with LAMP-5 therapeutic antibody (TAB-0643CL Creative Biolabs) and Anti-Mouse IgG Fc-DM1 Antibody with Non-Cleavable Linker (AM-103D1-50, Moradec LLC) at 5ng/uL and 1ng/uL final concentrations respectively. To measure cell viability CellTiter-Glo® 2.0 Cell Viability Assay (Promega Cat# G9242 WI, USA) was used following manufacture protocol.

SEAP reporters

THP-1-Blue NF-κB/ISG cells (InvivoGen) carrying a stable integrated NF-κB-inducible or ISG-inducible secreted embryonic alkaline phosphatase (SEAP) reporter construct were transduced with shLAMP5-2-Venus and sorted for Venus expression after 48 hours. Cells were then plated at a concentration of $2x10^4$ cells/well and stimulated with Pam3CSK4 (10ng/mL) or LPS (100ng/mL) for 24 hours. Cells were centrifuged and 20uL supernatant was incubated with 180uL QUANTI-Blue reagent at 37 degrees for 30 min - 2 hours. The levels of NF-κB-induced or ISG-induced SEAP was measured in a microplate reader at 620 nm.

Immunoflorescence

Cells seeded on alcian blue-treated coverslips were fixed with 3.5% PFA and permeabilized with 0.05% saponin. Cells were then stained overnight with primary antibodies: anti-LAMP-5 (Thermo Fisher Scientific Cat# 14-9778-80, RRID:AB_2573029), anti-MYD88 (R and D Systems Cat# AF2928, RRID:AB_2297977), anti-LAMP-1 BV421 (BioLegend Cat# 328626, RRID:AB_11203537) anti-LAMP-2 AF647 (Thermo Fisher Scientific Cat# A15464, RRID:AB_2534477). Immunofluorescence and confocal microscopy was performed with a Zeiss LSM580 63x objective and accompanying imaging softwares

Statistics

The statistical methodology used and sample sizes are described in the individual Figure legends. *t* tests were two tailed unless otherwise stated. Results are presented as mean ± SEM unless otherwise stated. A two-sided time-stratified Cochran-Mantel-Haenszel

was used for the Kaplan-Meier Survival analysis. ROC curves were used to determine the diagnostic utility of LAMP5 mRNA. The sensitivity and specificity were identified at the optimal cutoff point that was chosen at which the Youden's index was maximal. A significance level cutoff of 0.05 was used unless otherwise stated. Statistical analysis was performed using GraphPad Prism.

Authors Contributions:

G.G.M., L.H.L., and A.R.K. contributed to study conception and design. G.G.M., J.C., and D.L. acquired data. G.G.M., J.C., M.W., M.B., D.L., P.P., E.G., and L.H.L. analyzed and interpreted data. G.G.M., J.C., L.H.L. and A.R.K. wrote and revised the manuscript. M.W., D.L., P.P., E.G., reviewed the manuscript. M.W., D.L., and J.C., provided administrative, technical or material support.

Acknowledgments:

We would like to thank Daniel Starczcynowski, PhD, for his intellectual input. We would like to acknowledge the assistance of the Research Flow Cytometry Core in the Division of Rheumatology at Cincinnati Children’s Hospital Medical Center. All flow cytometric data were acquired using equipment maintained by the Research Flow Cytometry Core in the Division of Rheumatology at Cincinnati Children’s Hospital Medical Center.

M.W. was supported by an NIH grant (R50 CA211404). L.H.L. is a St. Baldrick’s Foundation Scholar and is supported by grants from CancerFree KIDS and the NIH (L40 HL143713-01) A.R.K. was supported by a Hyundai Hope on Wheels grant.

References

1. Ziemin-van der Poel S et al. Identification of a gene, MLL, that spans the breakpoint in 11q23 translocations associated with human leukemias. [Internet]. *Proc. Natl. Acad. Sci.* 1991;88(23):10735–10739.

2. Djabali M et al. A trithorax–like gene is interrupted by chromosome 11q23 translocations in acute leukaemias [Internet]. *Nat. Genet.* 1992;2(2):113–118.

3. Tkachuk DC, Kohler S, Cleary ML. Involvement of a homolog of Drosophila trithorax by 11q23 chromosomal translocations in acute leukemias [Internet]. *Cell* 1992;71(4):691–700.

4. Pui CH, Kane JR, Crist WM. Biology and treatment of infant leukemias.. *Leukemia* 1995;9:762–769.

5. Greaves MF. Infant leukaemia biology, aetiology and treatment. [Internet]. *Leukemia* 1996;10(2):372–7.

6. Meyer C et al. The MLL recombinome of acute leukemias in 2017 [Internet]. *Leukemia* 2018;32(2):273–284.

7. Hilden JM et al. Analysis of prognostic factors of acute lymphoblastic leukemia in infants: report on CCG 1953 from the Children's Oncology Group. [Internet]. *Blood* 2006;108(2):441–51.

8. Pieters R et al. A treatment protocol for infants younger than 1 year with acute lymphoblastic leukaemia (Interfant-99): an observational study and a multicentre randomised trial. [Internet]. *Lancet* 2007;370(9583):240–50.

9. Bauer J et al. Antigen Targets for the Development of Immunotherapies in Leukemia

527 [Internet]. *Int. J. Mol. Sci.* 2019;20(6):1397.

528 10. Rossi JG et al. Lineage switch in childhood acute leukemia: An unusual event with
529 poor outcome [Internet]. *Am. J. Hematol.* 2012;87(9):890–897.

530 11. Jacoby E et al. CD19 CAR immune pressure induces B-precursor acute
531 lymphoblastic leukaemia lineage switch exposing inherent leukaemic plasticity
532 [Internet]. *Nat. Commun.* 2016;7(1):12320.

533 12. Moschiano E, Raca G, Fu C, Pattengale PK, Oberley MJ. Congenital B-
534 lymphoblastic leukemia with a cryptic MLL rearrangement and post-treatment evolution
535 to mixed phenotype acute leukemia [Internet]. *Leuk. Res. Reports* 2016;6:29–32.

536 13. Rayes A, McMasters RL, O'Brien MM. Lineage Switch in MLL-Rearranged Infant
537 Leukemia Following CD19-Directed Therapy [Internet]. *Pediatr. Blood Cancer*
538 2016;63(6):1113–1115.

539 14. Haddox CL et al. Blinatumomab-induced lineage switch of B-ALL with
540 t(4:11)(q21;q23) KMT2A/AFF1 into an aggressive AML: pre- and post-switch
541 phenotypic, cytogenetic and molecular analysis [Internet]. *Blood Cancer J.*
542 2017;7(9):e607–e607.

543 15. Balducci E et al. Lineage switch from B acute lymphoblastic leukemia to acute
544 monocytic leukemia with persistent t(4;11)(q21;q23) and cytogenetic evolution under
545 CD19-targeted therapy [Internet]. *Ann. Hematol.* 2017;96(9):1579–1581.

546 16. Wölfl M et al. Spontaneous reversion of a lineage switch following an initial
547 blinatumomab-induced ALL-to-AML switch in MLL-rearranged infant ALL [Internet].
548 *Blood Adv.* 2018;2(12):1382–1385.

549 17. Aldoss I, Song JY. Extramedullary relapse of KMT2A(MLL)-rearranged acute
550 lymphoblastic leukemia with lineage switch following blinatumomab [Internet]. *Blood*
551 2018;131(22):2507–2507.

552 18. He RR et al. Immunotherapy- (Blinatumomab-) Related Lineage Switch of
553 KMT2A/AFF1 Rearranged B-Lymphoblastic Leukemia into Acute Myeloid
554 Leukemia/Myeloid Sarcoma and Subsequently into B/Myeloid Mixed Phenotype Acute
555 Leukemia [Internet]. *Case Rep. Hematol.* 2019;2019:1–4.

556 19. Duffner U et al. The possible perils of targeted therapy [Internet]. *Leukemia*
557 2016;30(7):1619–1621.

558 20. Winters AC, Bernt KM. MLL-Rearranged Leukemias—An Update on Science and
559 Clinical Approaches [Internet]. *Front. Pediatr.* 2017;5. doi:10.3389/fped.2017.00004

560 21. Wei J et al. Microenvironment Determines Lineage Fate in a Human Model of MLL-
561 AF9 Leukemia [Internet]. *Cancer Cell* 2008;13(6):483–495.

562 22. Cohen A, Petsche D, Grunberger T, Freedman MH. Interleukin 6 induces myeloid
563 differentiation of a human biphenotypic leukemic cell line [Internet]. *Leuk. Res.*
564 1992;16(8):751–760.

565 23. Bock T, Bausch-Fluck D, Hofmann A, Wollscheid B. CD proteome and beyond -
566 technologies for targeting the immune cell surfaceome. [Internet]. *Front. Biosci.*
567 *(Landmark Ed.* 2012;17(1):1599–612.

568 24. Hofmann A et al. Proteomic cell surface phenotyping of differentiating acute myeloid
569 leukemia cells [Internet]. *Blood* 2010;116(13):e26–e34.

570 25. Strassberger V et al. A comprehensive surface proteome analysis of myeloid

leukemia cell lines for therapeutic antibody development [Internet]. *J. Proteomics* 2014;99:138–151.

26. Hu CW et al. A quantitative analysis of heterogeneities and hallmarks in acute myelogenous leukaemia [Internet]. *Nat. Biomed. Eng.* 2019;3(11):889–901.

27. Mirkowska P et al. Leukemia surfaceome analysis reveals new disease-associated features [Internet]. *Blood* 2013;121(25):e149–e159.

28. Bausch-Fluck D et al. A Mass Spectrometric-Derived Cell Surface Protein Atlas [Internet]. *PLoS One* 2015;10(4):e0121314.

29. Bausch-Fluck D et al. The in silico human surfaceome [Internet]. *Proc. Natl. Acad. Sci.* 2018;115(46):E10988–E10997.

30. Zhou X et al. Exploring genomic alteration in pediatric cancer using ProteinPaint [Internet]. *Nat. Genet.* 2016;48(1):4–6.

31. Ma X et al. Pan-cancer genome and transcriptome analyses of 1,699 paediatric leukaemias and solid tumours [Internet]. *Nature* 2018;555(7696):371–376.

32. Haferlach T et al. Clinical Utility of Microarray-Based Gene Expression Profiling in the Diagnosis and Subclassification of Leukemia: Report From the International Microarray Innovations in Leukemia Study Group [Internet]. *J. Clin. Oncol.* 2010;28(15):2529–2537.

33. Armstrong SA et al. MLL translocations specify a distinct gene expression profile that distinguishes a unique leukemia [Internet]. *Nat. Genet.* 2002;30(1):41–47.

34. Zangrando A, Dell'Orto MC, te Kronnie G, Basso G. MLL rearrangements in pediatric acute lymphoblastic and myeloblastic leukemias: MLL specific and lineage

593 specific signatures [Internet]. *BMC Med. Genomics* 2009;2(1):36.

594 35. Ross ME et al. Gene expression profiling of pediatric acute myelogenous leukemia.
595 [Internet]. *Blood* 2004;104(12):3679–87.

596 36. Kroon E et al. Hoxa9 transforms primary bone marrow cells through specific
597 collaboration with Meis1a but not Pbx1b [Internet]. *EMBO J.* 1998;17(13):3714–3725.

598 37. Shen WF et al. AbdB-like Hox proteins stabilize DNA binding by the Meis1
599 homeodomain proteins. [Internet]. *Mol. Cell. Biol.* 1997;17(11):6448–6458.

600 38. Lawrence HJ et al. Mice bearing a targeted interruption of the homeobox gene
601 HOXA9 have defects in myeloid, erythroid, and lymphoid hematopoiesis. [Internet].
602 *Blood* 1997;89(6):1922–30.

603 39. Lawrence HJ et al. Loss of expression of the Hoxa-9 homeobox gene impairs the
604 proliferation and repopulating ability of hematopoietic stem cells. [Internet]. *Blood*
605 2005;106(12):3988–94.

606 40. Kumar AR et al. Hoxa9 influences the phenotype but not the incidence of Mll-AF9
607 fusion gene leukemia. *Blood* 2004;103(5):1823–1828.

608 41. Unnisa Z et al. Meis1 preserves hematopoietic stem cells in mice by limiting
609 oxidative stress. [Internet]. *Blood* 2012;120(25):4973–81.

610 42. Kumar AR et al. A role for MEIS1 in MLL-fusion gene leukemia. [Internet]. *Blood*
611 2009;113(8):1756–8.

612 43. Roychoudhury J et al. MEIS1 regulates an HLF-oxidative stress axis in MLL-fusion
613 gene leukemia. [Internet]. *Blood* 2015;125(16):2544–52.

614 44. Valk PJ et al. Prognostically Useful Gene-Expression Profiles in Acute Myeloid
615 Leukemia [Internet]. *N. Engl. J. Med.* 2004;350(16):1617–1628.

616 45. Stam RW et al. Gene expression profiling-based dissection of MLL translocated and
617 MLL germline acute lymphoblastic leukemia in infants [Internet]. *Blood*
618 2010;115(14):2835–2844.

619 46. Lavallée V-P et al. The transcriptomic landscape and directed chemical interrogation
620 of MLL-rearranged acute myeloid leukemias [Internet]. *Nat. Genet.* 2015;47(9):1030–
621 1037.

622 47. David A et al. BAD-LAMP defines a subset of early endocytic organelles in
623 subpopulations of cortical projection neurons [Internet]. *J. Cell Sci.* 2007;120(2):353–
624 365.

625 48. Tiveron M-C et al. LAMP5 Fine-Tunes GABAergic Synaptic Transmission in Defined
626 Circuits of the Mouse Brain [Internet]. *PLoS One* 2016;11(6):e0157052.

627 49. Koebis M et al. LAMP5 in presynaptic inhibitory terminals in the hindbrain and spinal
628 cord: a role in startle response and auditory processing [Internet]. *Mol. Brain*
629 2019;12(1):20.

630 50. Defays A et al. BAD-LAMP is a novel biomarker of nonactivated human
631 plasmacytoid dendritic cells [Internet]. *Blood* 2011;118(3):609–617.

632 51. Villani A et al. Single-cell RNA-seq reveals new types of human blood dendritic
633 cells, monocytes, and progenitors [Internet]. *Science (80-.).* 2017;356(6335):eaah4573.

634 52. Combes A et al. BAD-LAMP controls TLR9 trafficking and signalling in human
635 plasmacytoid dendritic cells [Internet]. *Nat. Commun.* 2017;8(1):913.

53. Gu Z et al. PAX5-driven subtypes of B-progenitor acute lymphoblastic leukemia [Internet]. *Nat. Genet.* 2019;51(2):296–307.

54. Otzen Bagger F et al. BloodSpot: a database of gene expression profiles and transcriptional programs for healthy and malignant haematopoiesis [Internet]. *Nucleic Acids Res.* 2015;44:917–924.

55. Wilkinson AC et al. RUNX1 Is a Key Target in t(4;11) Leukemias that Contributes to Gene Activation through an AF4-MLL Complex Interaction [Internet]. *Cell Rep.* 2013;3(1):116–127.

56. Benito JM et al. MLL-Rearranged Acute Lymphoblastic Leukemias Activate BCL-2 through H3K79 Methylation and Are Sensitive to the BCL-2-Specific Antagonist ABT-199 [Internet]. *Cell Rep.* 2015;13(12):2715–2727.

57. Wang Q-F et al. MLL fusion proteins preferentially regulate a subset of wild-type MLL target genes in the leukemic genome. [Internet]. *Blood* 2011;117(25):6895–905.

58. Lin S et al. Instructive Role of MLL-Fusion Proteins Revealed by a Model of t(4;11) Pro-B Acute Lymphoblastic Leukemia [Internet]. *Cancer Cell* 2016;30(5):737–749.

59. Mirantes C, Passegué E, Pietras EM. Pro-inflammatory cytokines: Emerging players regulating HSC function in normal and diseased hematopoiesis [Internet]. *Exp. Cell Res.* 2014;329(2):248–254.

60. Hemmati S, Haque T, Gritsman K. Inflammatory Signaling Pathways in Preleukemic and Leukemic Stem Cells [Internet]. *Front. Oncol.* 2017;7:265.

61. Cohen P. The TLR and IL-1 signalling network at a glance [Internet]. *J. Cell Sci.* 2014;127(11):2383–2390.

62. Kuo H-P et al. Epigenetic Roles of MLL Oncoproteins Are Dependent on NF-κB [Internet]. *Cancer Cell* 2013;24(4):423–437.

63. Liang K et al. Therapeutic Targeting of MLL Degradation Pathways in MLL-Rearranged Leukemia. [Internet]. *Cell* 2017;168(1–2):59-72.e13.

64. Deguine J, Barton GM. MyD88: a central player in innate immune signaling [Internet]. *F1000Prime Rep.* 2014;6:97.

65. Eriksson M et al. Agonistic targeting of TLR1/TLR2 induces p38 MAPK-dependent apoptosis and NFκB-dependent differentiation of AML cells [Internet]. *Blood Adv.* 2017;1(23):2046–2057.

66. Mercurio F. IKK-1 and IKK-2: Cytokine-Activated IB Kinases Essential for NF-B Activation [Internet]. *Science (80-.).* 1997;278(5339):860–866.

67. Cui J et al. NLRC5 Negatively Regulates the NF-κB and Type I Interferon Signaling Pathways [Internet]. *Cell* 2010;141(3):483–496.

68. Wang W-T et al. Activation of the Lysosome-Associated Membrane Protein LAMP5 by DOT1L Serves as a Bodyguard for MLL Fusion Oncoproteins to Evade Degradation in Leukemia [Internet]. *Clin. Cancer Res.* 2019;25(9):2795–2808.

69. Ning S, Pagano JS, Barber GN. IRF7: activation, regulation, modification and function [Internet]. *Genes Immun.* 2011;12(6):399–414.

70. Kannan K et al. Lysosome-Associated Membrane Proteins h-LAMP1 (CD107a) and h-LAMP2 (CD107b) Are Activation-Dependent Cell Surface Glycoproteins in Human Peripheral Blood Mononuclear Cells Which Mediate Cell Adhesion to Vascular Endothelium [Internet]. *Cell. Immunol.* 1996;171(1):10–19.

71. Ramprasad MP, Terpstra V, Kondratenko N, Quehenberger O, Steinberg D. Cell surface expression of mouse macrosialin and human CD68 and their role as macrophage receptors for oxidized low density lipoprotein [Internet]. *Proc. Natl. Acad. Sci.* 1996;93(25):14833–14838.

72. de Saint-Vis B et al. A Novel Lysosome-Associated Membrane Glycoprotein, DC-LAMP, Induced upon DC Maturation, Is Transiently Expressed in MHC Class II Compartment [Internet]. *Immunity* 1998;9(3):325–336.

73. Leone DA et al. Surface LAMP-2 Is an Endocytic Receptor That Diverts Antigen Internalized by Human Dendritic Cells into Highly Immunogenic Exosomes [Internet]. *J. Immunol.* 2017;199(2):531–546.

74. Oosenbrug T, van de Graaff MJ, Ressing ME, van Kasteren SI. Chemical Tools for Studying TLR Signaling Dynamics [Internet]. *Cell Chem. Biol.* 2017;24(7):801–812.

75. Tracey L et al. NF-κB activation mediates resistance to IFNβ in MLL-rearranged acute lymphoblastic leukemia [Internet]. *Leukemia* 2010;24(4):806–812.

76. Furuta K, Yang X-L, Chen J-S, Hamilton SR, August JT. Differential Expression of the Lysosome-Associated Membrane Proteins in Normal Human Tissues [Internet]. *Arch. Biochem. Biophys.* 1999;365(1):75–82.

77. Chistiakov DA, Killingsworth MC, Myasoedova VA, Orekhov AN, Bobryshev Y V. CD68/macrosialin: not just a histochemical marker [Internet]. *Lab. Investig.* 2017;97(1):4–13.

78. Beird HC et al. Features of non-activation dendritic state and immune deficiency in blastic plasmacytoid dendritic cell neoplasm (BPDCN) [Internet]. *Blood Cancer J.*

2019;9(12):99.

79. Ledergor G et al. Single cell dissection of plasma cell heterogeneity in symptomatic and asymptomatic myeloma [Internet]. *Nat. Med.* 2018;24(12):1867–1876.

80. Xu Y et al. Toll-like Receptor 4 Is a Sensor for Autophagy Associated with Innate Immunity [Internet]. *Immunity* 2007;27(1):135–144.

81. Delgado MA, Elmaoued RA, Davis AS, Kyei G, Deretic V. Toll-like receptors control autophagy [Internet]. *EMBO J.* 2008;27(7):1110–1121.

82. Anand PK et al. TLR2 and RIP2 Pathways Mediate Autophagy of Listeria monocytogenes via Extracellular Signal-regulated Kinase (ERK) Activation [Internet]. *J. Biol. Chem.* 2011;286(50):42981–42991.

83. Into T, Inomata M, Takayama E, Takigawa T. Autophagy in regulation of Toll-like receptor signaling [Internet]. *Cell. Signal.* 2012;24(6):1150–1162.

84. Franco LH et al. Autophagy downstream of endosomal Toll-like receptor signaling in macrophages is a key mechanism for resistance to Leishmania major infection [Internet]. *J. Biol. Chem.* 2017;292(32):13087–13096.

85. Rothe K, Porter V, Jiang X. Current Outlook on Autophagy in Human Leukemia: Foe in Cancer Stem Cells and Drug Resistance, Friend in New Therapeutic Interventions [Internet]. *Int. J. Mol. Sci.* 2019;20(3):461.

86. Watson A et al. Autophagy limits proliferation and glycolytic metabolism in acute myeloid leukemia [Internet]. *Cell Death Discov.* 2015;1(1):15008.

87. Liu Q, Chen L, Atkinson JM, Claxton DF, Wang H-G. Atg5-dependent autophagy contributes to the development of acute myeloid leukemia in an MLL-AF9-driven mouse

model [Internet]. *Cell Death Dis.* 2016;7(9):e2361–e2361.

88. Sumitomo Y et al. Cytoprotective autophagy maintains leukemia-initiating cells in murine myeloid leukemia [Internet]. *Blood* 2016;128(12):1614–1624.

89. Chen X et al. Autophagy is dispensable for *Kmt2a/Mll-Mllt3/Af9* AML maintenance and anti-leukemic effect of chloroquine [Internet]. *Autophagy* 2017;13(5):955–966.

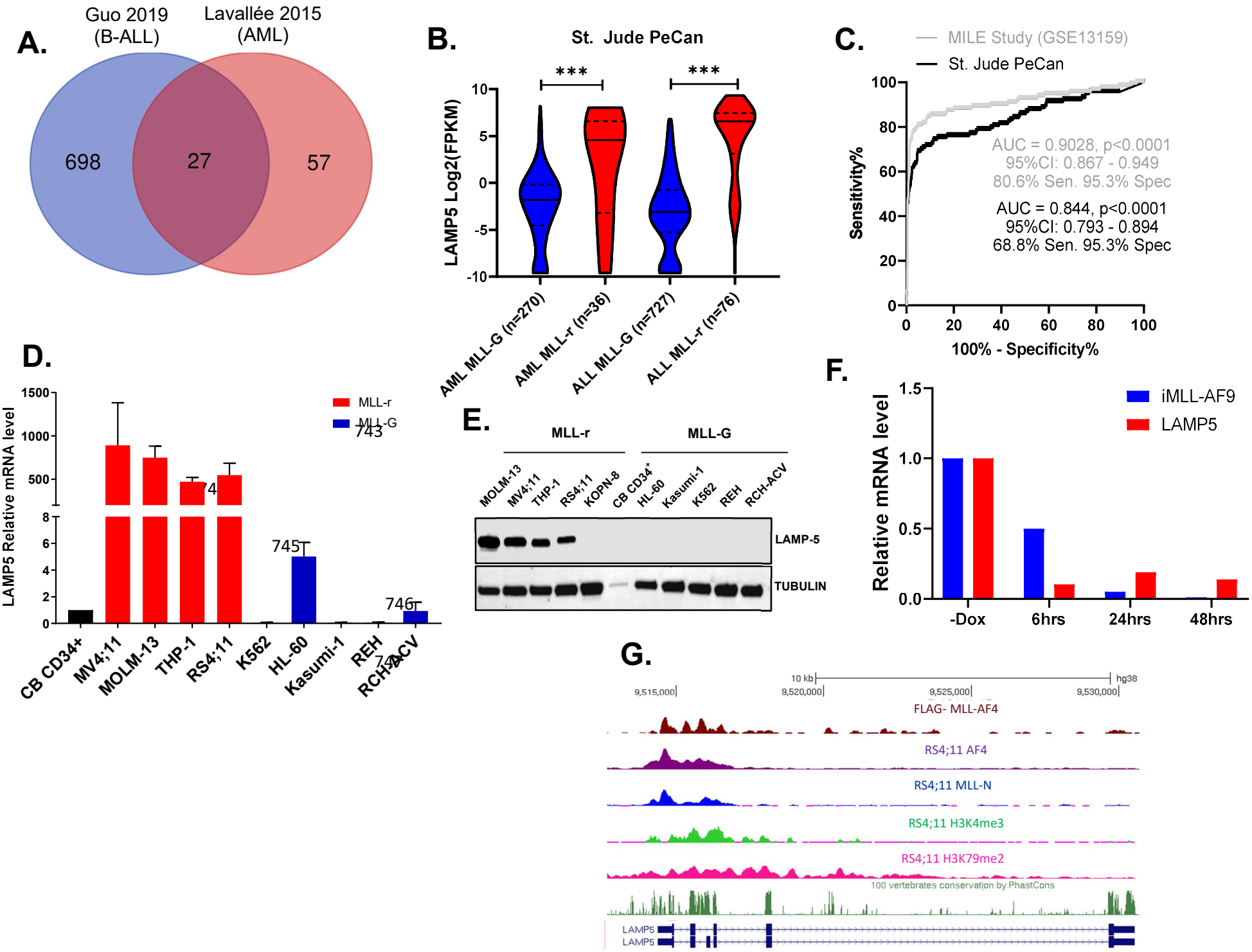
A.
Guo 2019
(B-ALL)
Lavallée 2015
(AML)
698
27
57
B.
St. Jude PeCan
LAMP5 Log2(FPKM)
***
***
AML MLL-G (n=270)
AML MLL-r (n=36)
ALL MLL-G (n=727)
ALL MLL-r (n=76)
C.
MILE Study (GSE13159)
St. Jude PeCan
Sensitivity%
100% - Specificity%
AUC = 0.9028, p<0.0001
95%CI: 0.867 - 0.949
80.6% Sen. 95.3% Spec
AUC = 0.844, p<0.0001
95%CI: 0.793 - 0.894
68.8% Sen. 95.3% Spec
D.
LAMP5 Relative mRNA level
MLL-r
MLL-G
743
745
746
CB CD34+
MV4;11
MOLM-13
THP-1
RS4;11
K562
HL-60
Kasumi-1
REH
RCH-ACV
E.
MLL-r
MLL-G
MOLM-13
MV4;11
THP-1
RS4;11
KOPN-8
CB CD34+
HL-60
Kasumi-1
K562
REH
RCH-ACV
LAMP-5
TUBULIN
F.
Relative mRNA level
iMLL-AF9
LAMP5
-Dox
6hrs
24hrs
48hrs
G.
10 kb
hg38
9,515,000
9,520,000
9,525,000
9,530,000
FLAG- MLL-AF4
RS4;11 AF4
RS4;11 MLL-N
RS4;11 H3K4me3
RS4;11 H3K79me2
100 vertebrates conservation by PhastCons
LAMP5
LAMP5

Figure 1: *LAMP5* is highly expressed in MLL-r leukemias and is a direct target of the MLL-fusion protein (MLL-FP). (A) Intersection of published gene expression signatures composed of genes overexpressed in MLL-rearranged AML and ALL when compared to MLL-Germline leukemias. **(B)** Log2 FPKM expression of *LAMP5* in AML and ALL pediatric patients with MLL-rearrangement (AML MLL-r, n=36 and ALL MLL-r, n=76) compared to MLL-Germline (AML MLL-G, n=270) (ALL MLL-G, n=727) patients. Data obtained from the St. Jude PeCan Portal and presented as median value with quartiles (*t*- test, p< 0.0001**) (C)** Receiving Operating Curve (ROC) analysis showing capacity of *LAMP5* to discriminate acute leukemia patients with MLL-Germ or MLL-r leukemias. Data obtained from GSE13159 and St. Jude Pecan Portal **(D)** Relative expression of *LAMP5* in MLL-r leukemia (MV4;11, MOLM-13, KOPN-8, THP-1 and RS4;11) and MLL-Germ leukemia (K562, HL-60, Kasumi-1, REH, RCH-ACV) cell lines. The graph represents relative expression of *LAMP5* normalized to *B-ACTIN*. Data is from 3 biological replicates. *LAMP5* expression in cord blood cells was set as 1.0. Bars show mean ± SEM. **(E)** Western blot analysis of the LAMP-5 levels in MLL-r leukemia and MLL-Germ leukemia human cell lines. $CD34^+$ cord blood cells were used as control. TUBULIN was used as a loading control. **(F)** Graph represents the relative expression of *LAMP5* and *MLL-AF9* upon incubation with Doxycycline. Relative expression of *LAMP5* and *MLL-AF9* normalized to *B-ACTIN*. **(G)** ChIP-seq profiles of human ALL cell lines expressing MLL-AF4 show binding of the MLL N-terminus, AF4 C-terminus and significant H3K4me3 and H3K79me2 mark in the *LAMP5* promoter and gene body. ChIP-seq data were obtained for the CB $CD34^+$ transformed with MLL-Af4 and RS4;11 from GSE84116 and GSE38403 respectively.

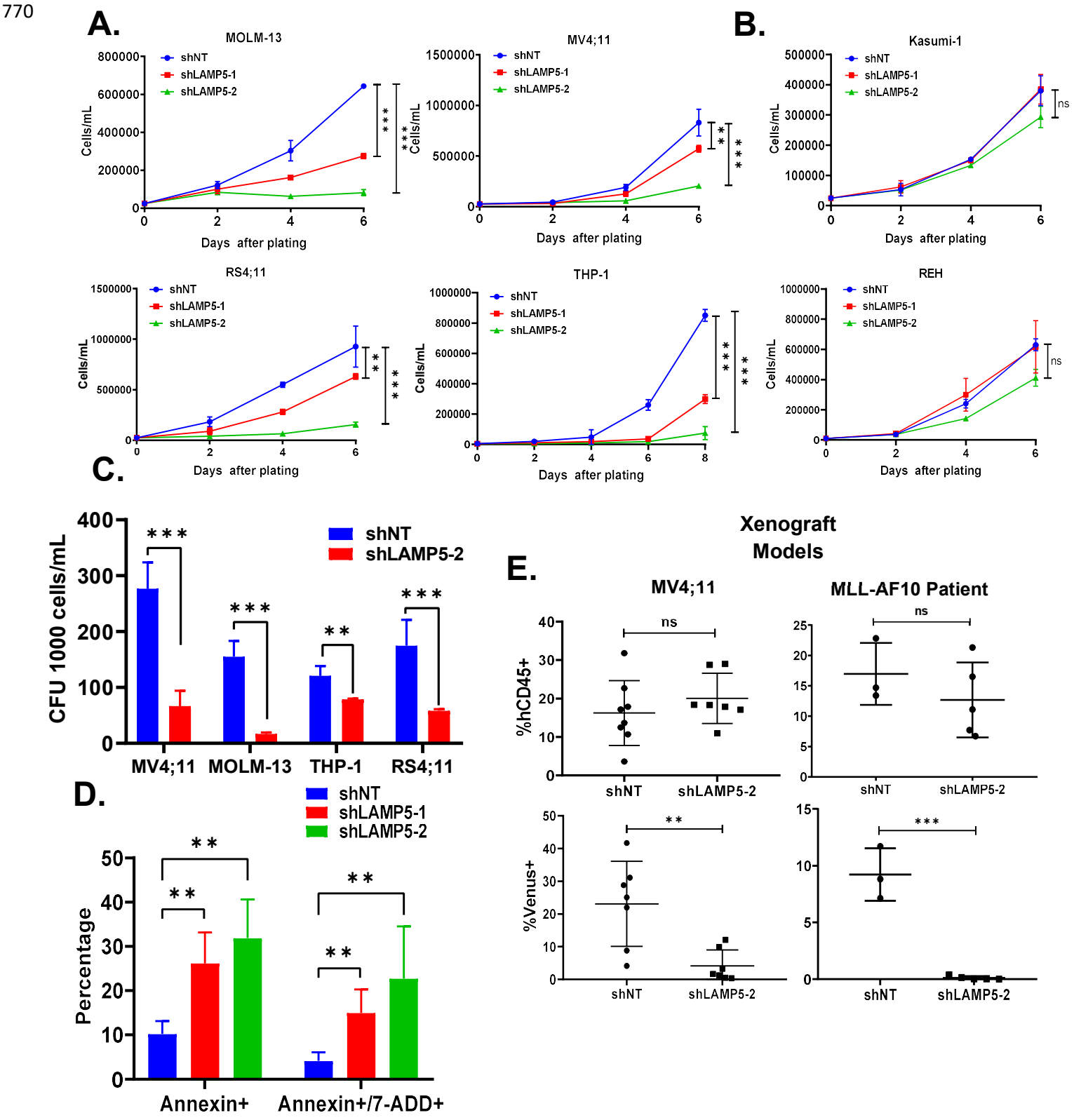
A.
MOLM-13
MV4;11
B.
Kasumi-1
RS4;11
THP-1
REH
shNT
shLAMP5-1
shLAMP5-2
Cells/mL
Days after plating
ns
C.
CFU 1000 cells/mL
MV4;11
MOLM-13
THP-1
RS4;11
D.
Percentage
Annexin+
Annexin+/7-ADD+
E.
Xenograft Models
MV4;11
MLL-AF10 Patient
%hCD45+
%Venus+

Figure 2: LAMP5 expression is required for MLL-r leukemia survival *in vitro* and *in vivo*. (A-B) *In vitro* growth of MLL-r and MLL-G leukemia cell lines **(A)** (MOLM-13, MV4;11, RS4;11 and THP-1) and **(B)** (Kasumi-1 and REH) respectively upon shRNA knockdown of *LAMP5*. Data are from 3 independent experiments, *t* test, (**,p<0.01, ***, p< 0.001). **(C)** Colony forming units (CFU) of MV4;11 and MOLM-13 cells upon *LAMP5* shRNA knockdown. Data are from 3 biological replicates, represented as mean and SEM (**,p<0.01, ***, p< 0.001). **(D)** Percentage of Annexin$^+$ or Annexin$^+$/7-AAD$^+$ cells after transduction with shNT, shLAMP5-1 and shLAMP5-2. Data are from 3 biological replicates, represented as mean and SEM of at least 3 experiments. *t* test, p< 0.01 **(E)** Plots show percentage of human CD45$^+$ (upper) and Venus$^+$ cells in the CD45$^+$ fraction (lower) in MV4;11 (left) and MLL-AF10 primary patient sample (right). Data are from 8 biological replicates for MV4;11 and 5 biological replicates for the MLL-AF10 primary patient, represented as mean and SEM. *t* test, p< 0.01

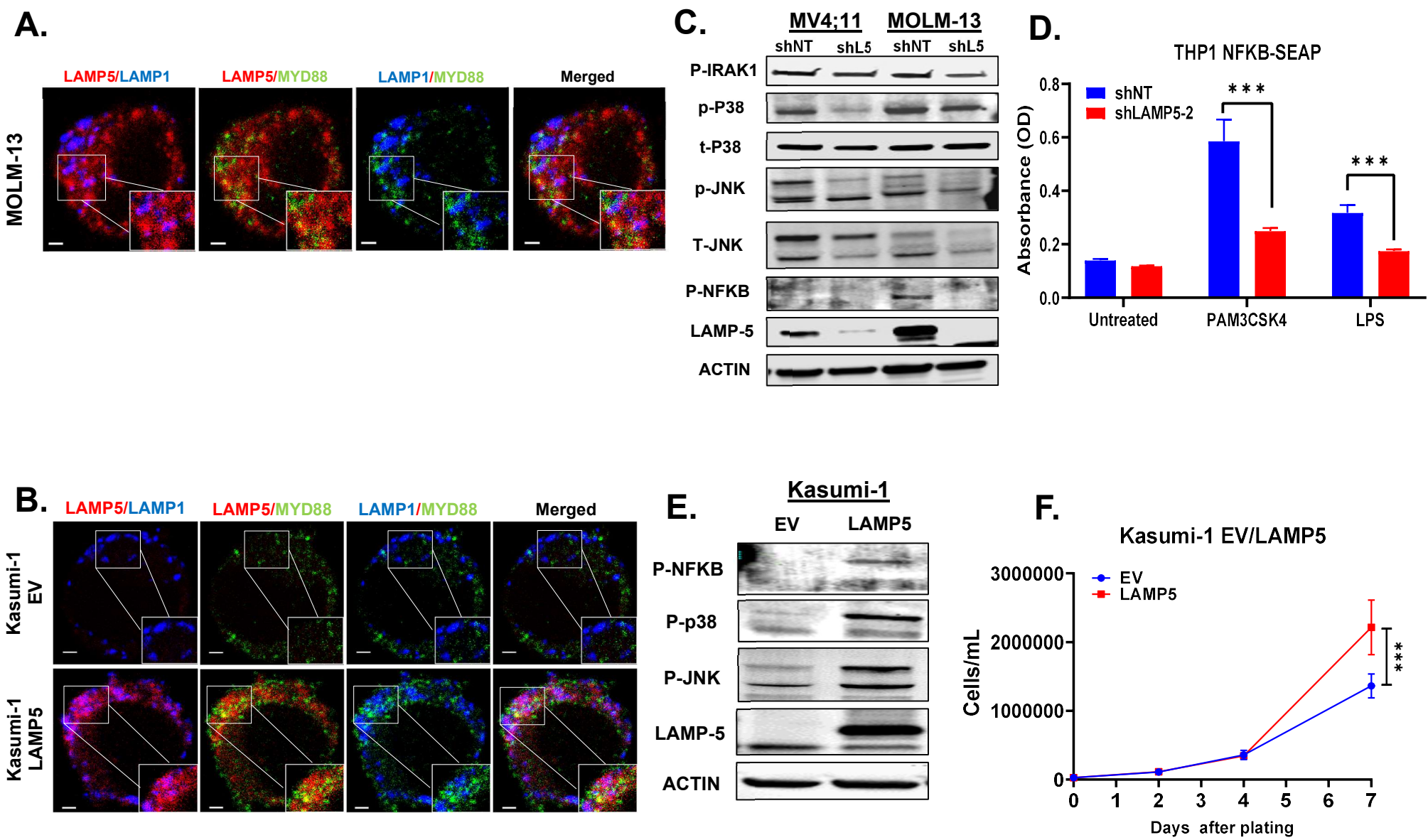
A.
LAMP5/LAMP1
LAMP5/MYD88
LAMP1/MYD88
Merged
MOLM-13
B.
LAMP5/LAMP1
LAMP5/MYD88
LAMP1/MYD88
Merged
Kasumi-1 EV
Kasumi-1 LAMP5
C.
MV4;11
MOLM-13
shNT
shL5
shNT
shL5
P-IRAK1
p-P38
t-P38
p-JNK
T-JNK
P-NFKB
LAMP-5
ACTIN
D.
THP1 NFKB-SEAP
shNT
shLAMP5-2
Absorbance (OD)
0.8
0.6
0.4
0.2
0.0
***
***
Untreated
PAM3CSK4
LPS
E.
Kasumi-1
EV
LAMP5
P-NFKB
P-p38
P-JNK
LAMP-5
ACTIN
F.
Kasumi-1 EV/LAMP5
EV
LAMP5
Cells/mL
3000000
2000000
1000000
0
***
0
1
2
3
4
5
6
7
Days after plating

Figure 3: LAMP-5 is required for activation of TLR/IL1R signaling (A) Representative confocal microscopy images showing MV4;11 cells stained with LAMP-5, LAMP-1 and MYD88. Scale bar = 1µm **(B)** Confocal microscopy image showing Kasumi-1 cells overexpressing EV or *LAMP5* stained with LAMP-5, LAMP-2 and MYD88. Scale bar = 1µm **(C)** Western blot analysis showing that LAMP-5 depletion (shL5) led to a decrease of p-IRAK1, p-p38, p-JNK, and p-NFKB, known downstream targets of TLR signaling. **(D)** THP-1-Blue-NFKB reporter cell line was treated with PAM3CSK2 10ng/mL or LPS 100ng/mL in the presence or absence of LAMP5. Data are from 3 independent experiments t-test, ***, $p < 0.001$. **(E)** Western blot analysis showing Kasumi-1 cells with overexpression of EV or *LAMP5* showing increase activation of p-NFKB, p-p38 and p-JNK. **(F)** *In vitro* cell growth of Kasumi-1 cells overexpressing EV or LAMP5. Data are from 3 individual experiments, t-test, ***, $p < 0.001$.

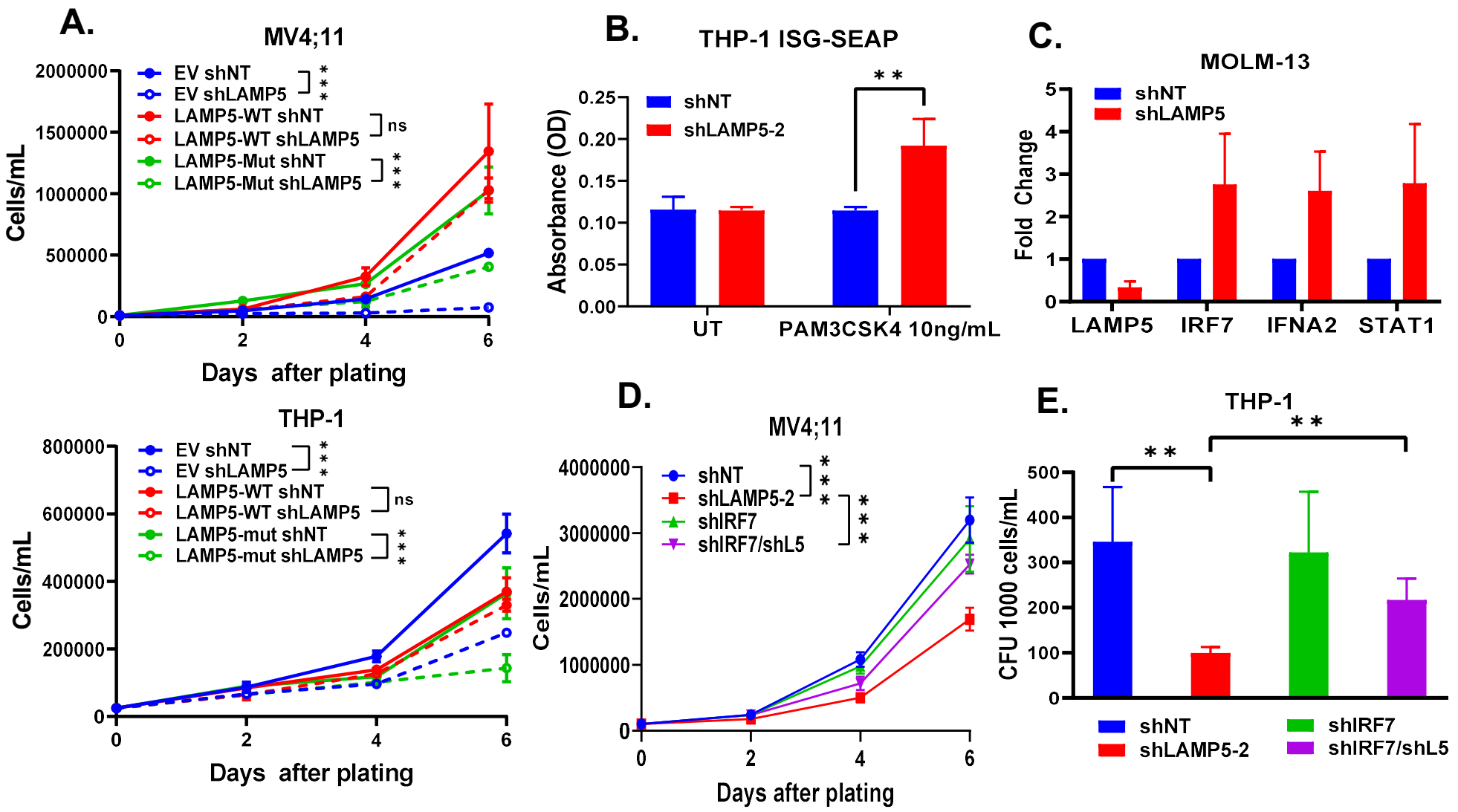
A.
MV4;11
Cells/mL
Days after plating
EV shNT
EV shLAMP5
LAMP5-WT shNT
LAMP5-WT shLAMP5
LAMP5-Mut shNT
LAMP5-Mut shLAMP5
ns
THP-1
LAMP5-mut shNT
LAMP5-mut shLAMP5
B.
THP-1 ISG-SEAP
Absorbance (OD)
shNT
shLAMP5-2
UT
PAM3CSK4 10ng/mL
C.
MOLM-13
Fold Change
shLAMP5
LAMP5
IRF7
IFNA2
STAT1
D.
MV4;11
shIRF7
shIRF7/shL5
E.
THP-1
CFU 1000 cells/mL

Figure 4: LAMP5 is a negative regulator of IFN-1 signaling in MLL-r leukemias (A) In-vitro growth of MV4;11 and THP-1 cells overexpressing EV, LAMP-5 WT, or LAMP-5-mut upon shRNA knockdown of LAMP-5. Data are from 3 independent experiments. t-test ***, p< 0.001. **(B)** THP-1 ISG blue reporter cell line was treated with 10ng/mL PAM3CSK2 in the presence or absence of LAMP-5. Data are from 3 independent experiments. Bars show mean ± SEM. t-test **,p<0.01. **(C)** Relative expression of *LAMP5*, *IRF7, IFNA2* and *STAT1* upon knockdown of LAMP-5 in MOLM-13 cells**.** The graph represents relative expression of *LAMP5*, *IRF7*, *IFNA2*, and *STAT1* normalized to *β-ACTIN*. Data are from 3 biological replicates. Bars show mean ± SEM. **(D)** *In vitro* growth of MV4;11 after LAMP5, or IRF7 or LAMP5 and IRF7 shRNA knockdown. Data are from 3 independent experiments, represented as mean and ±SD. ***, p< 0.001. **(E)** Colony forming units (CFU) of THP-1 cells upon shRNA knockdown of LAMP-5, IRF7, or LAMP-5 and IRF7 together. Data are from 3 independent experiment, represented as mean and ±SD, t-test **,p<0.01.

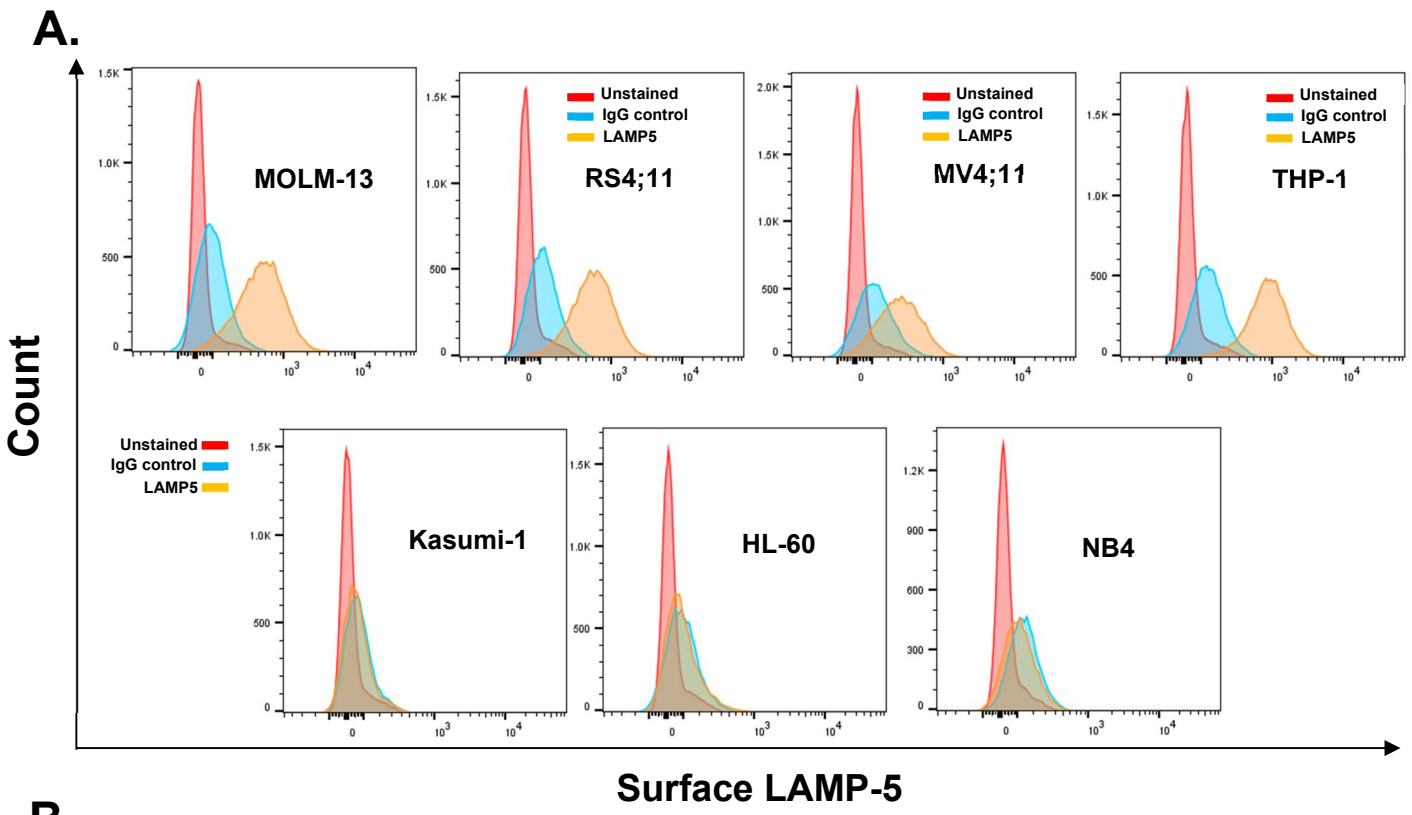
A.
Count
MOLM-13
RS4;11
MV4;11
THP-1
Kasumi-1
HL-60
NB4
Unstained
IgG control
LAMP5
Surface LAMP-5

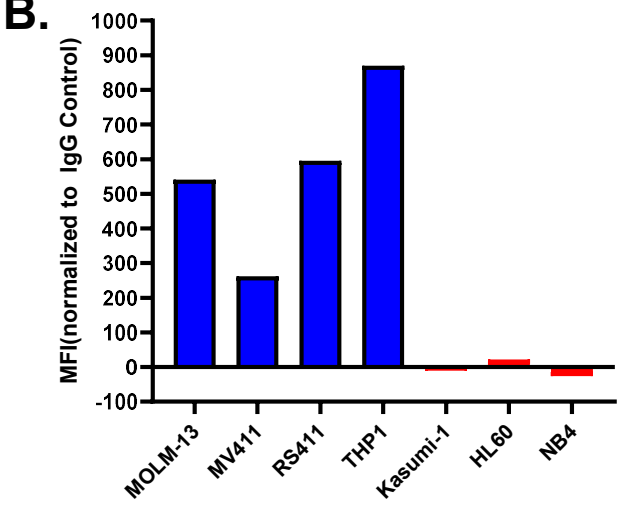
B.
MFI(normalized to IgG Control)
MOLM-13
MV411
RS411
THP1
Kasumi-1
HL60
NB4

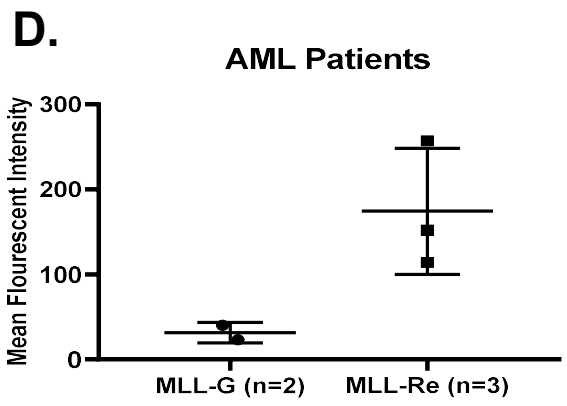
D.
AML Patients
Mean Flourescent Intensity
MLL-G (n=2)
MLL-Re (n=3)

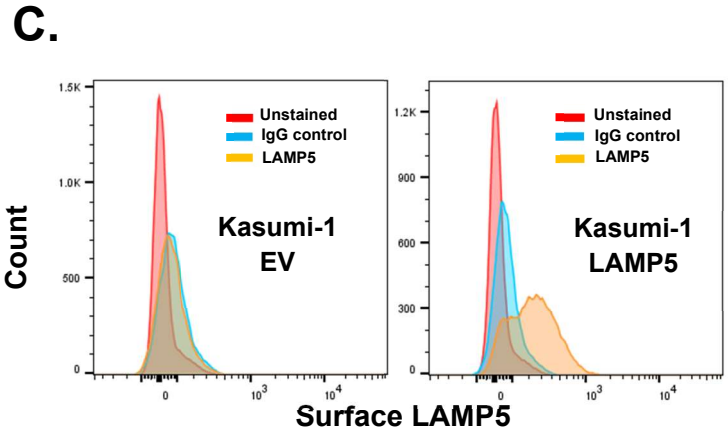
C.
Count
Kasumi-1
EV
Kasumi-1
LAMP5
Unstained
IgG control
LAMP5
Surface LAMP5

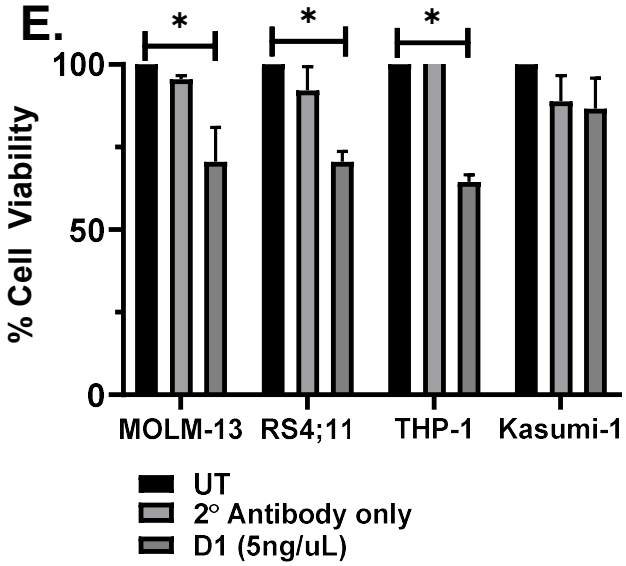
E.
% Cell Viability
MOLM-13
RS4;11
THP-1
Kasumi-1
UT
2° Antibody only
D1 (5ng/uL)

Figure 5: Surface LAMP-5 can be detected and targeted with Antibody Drug Conjugate therapy

(A) Representative histogram plots showing LAMP-5 surface expression in MLL-r leukemia (MOLM-13, RS4;11, MV4;11, and THP-1) and MLL-Germ leukemia (Kasumi-1, HL-60 and NB4) cell lines **(B)** Graph showing mean fluorescence intensity (MFI) of LAMP-5 surface staining in MLL-r leukemias vs MLL-Germ leukemias. **(C)** Representative histogram of LAMP-5 staining in Kasumi-1 expressing EV or LAMP5, confirming the specificity of the antibody. (**D)** MFI of LAMP-5 surface expression in MLL-r and MLL-Germ AML patients. **(E)** MOLM-13, RS4;11, THP-1 and Kasumi-1 cells were incubated with surface LAMP-5 antibody clone D1 and αMFc-NC-DM1 ADC antibody for 72h. Bar graph represents cell viability from 3 biological replicates presented as Mean and ±SEM

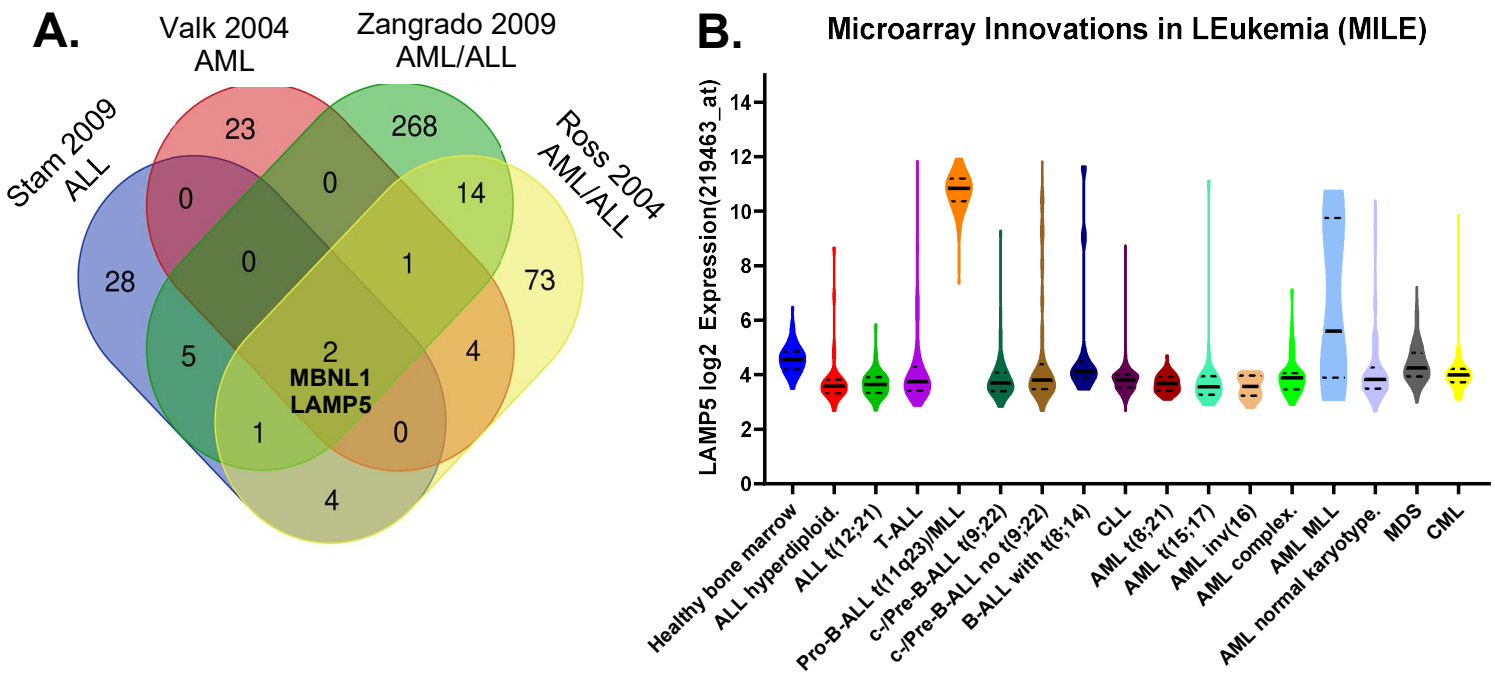

Supplemental Figure 1: (A) Intersection of published gene expression signatures composed of genes overexpressed in MLL-rearranged AML and ALL when compared to other MLL-germline leukemias. **(B)** Log2 microarray expression of *LAMP5* in multiple molecular subtypes of leukemia from the Microarray Innovations in Leukemia (MILE) Study. Data shown as median values and quartiles. Normalized data from Bloodspot.eu

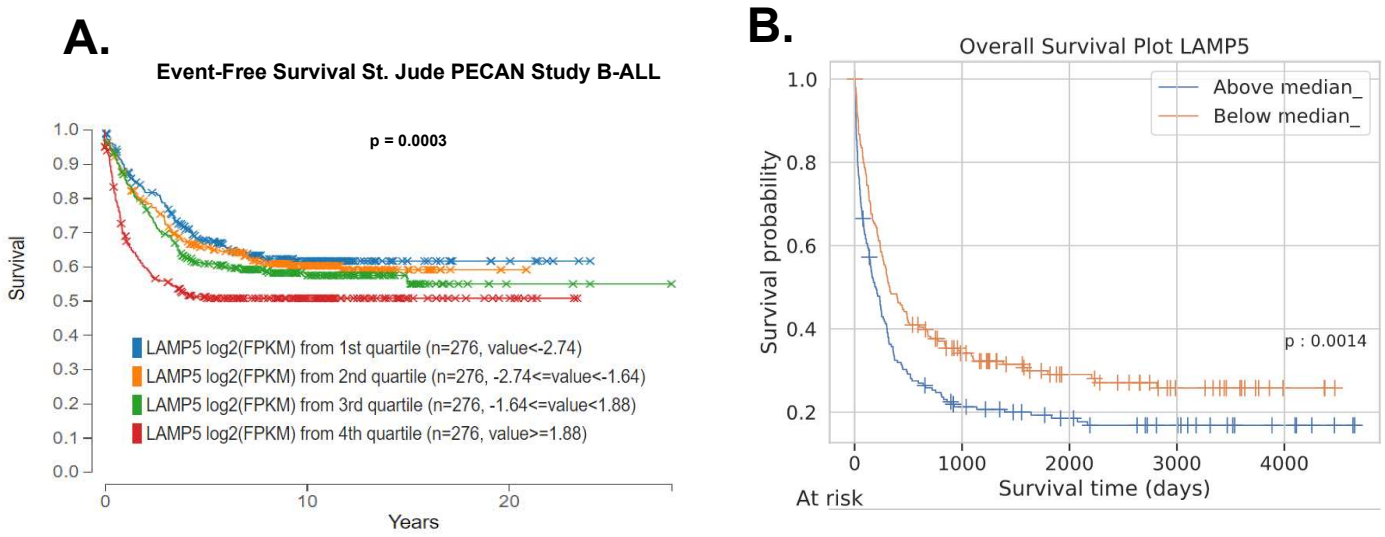

Supplemental Figure 2: (A) Kaplan-Meier Event-free survival curve of B-ALL patients based on *LAMP5* Log_2(FPKM) expression (n=1,104 two-sided time-stratified Cochran–Mantel–Haenszel test p=0.003). Data obtained from the St. Jude PeCan Portal. (**B)** Kaplan-Meier Overall survival curve of AML patients based on *LAMP5* (TPM) expression (n=374 two-sided time-stratified Cochran–Mantel–Haenszel test p=0.0014). Data obtained from the Leucegene Data Portal.

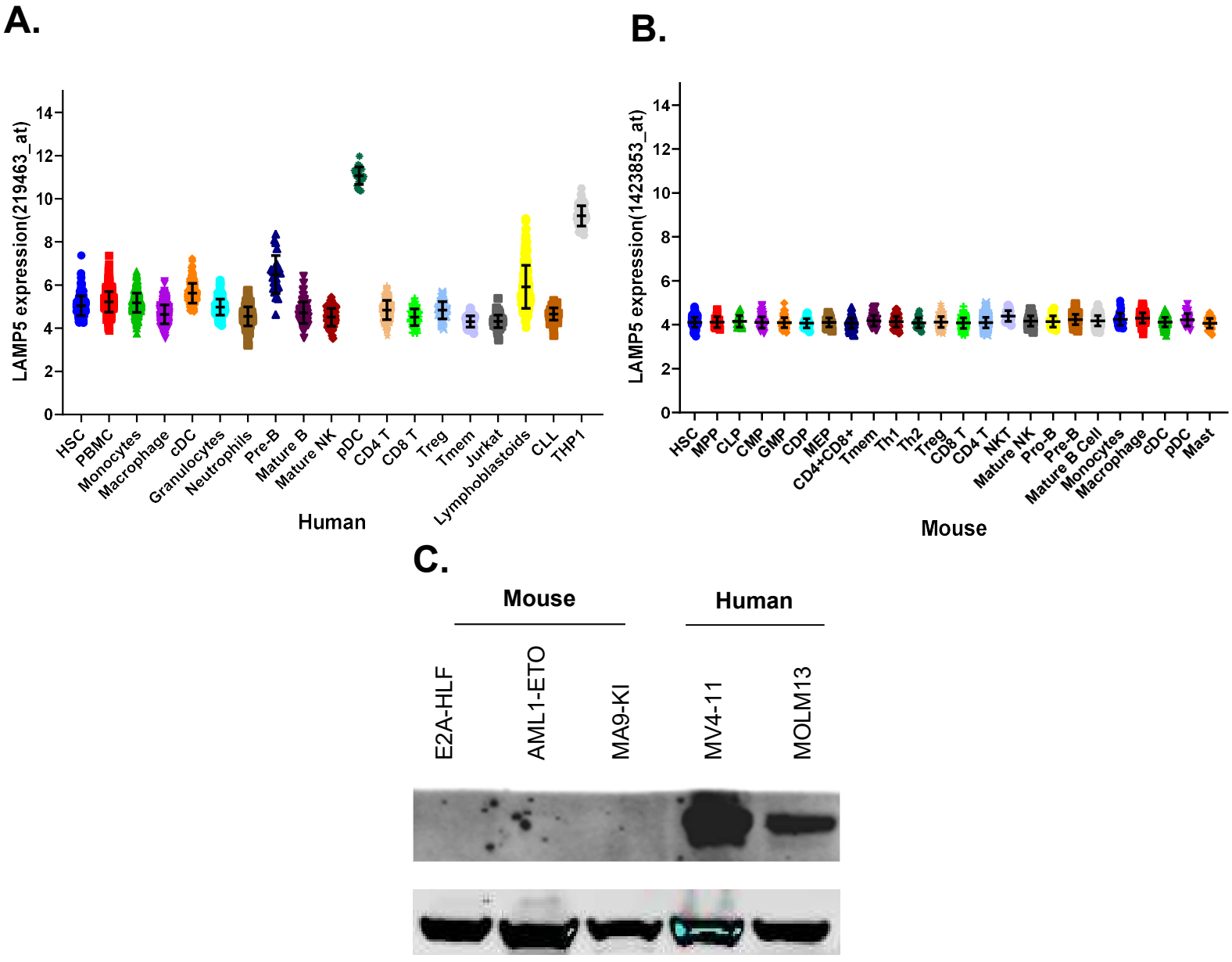

Supplemental Figure 3: (A) Normalized Microarray expression data of LAMP5 in human blood and leukemia (THP-1 as MLL-AF9 control). Data from Immuno-Navigator portal, presented as Mean with SD. **(B)** Normalized Microarray expression data of *Lamp5* in mouse blood. Data from Immuno-Navigator portal, presented as Mean with SD. **(C)** Western blot analysis of LAMP-5 expression in Mouse Lin(-) cells transformed with E2A-HLF, AML1-ETO, MLL-AF9. MV4-11 and MOLM-13 cells were used as control.

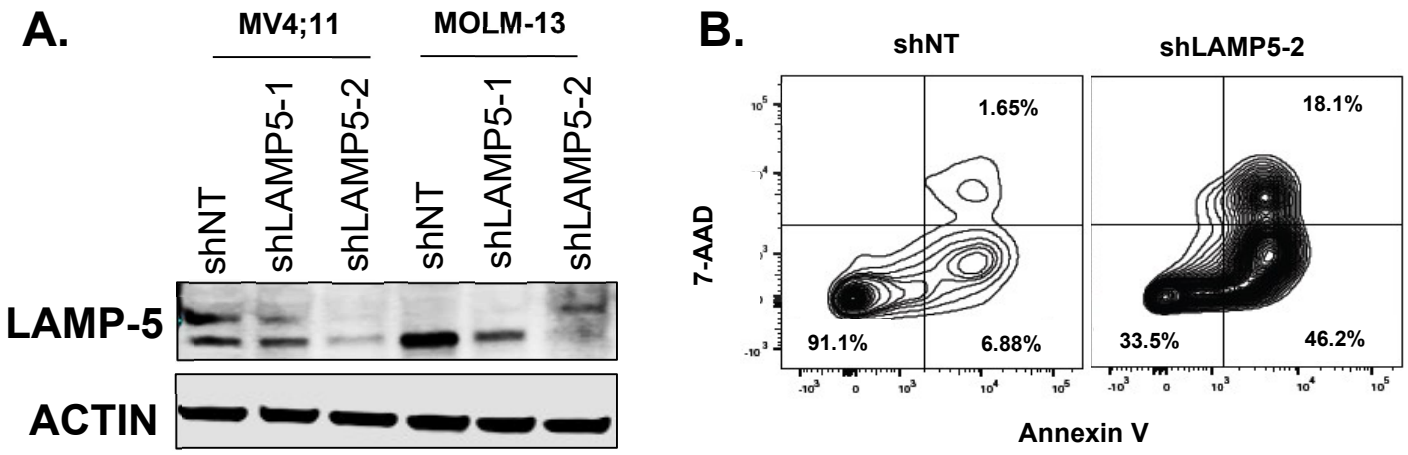

Supplemental Figure 4: (A) Western blot analysis of LAMP-5 expression in MV4;11 and MOLM-13 cells after transduction of shLAMP5-1 and shLAMP5-2. **(B)** Representative contour plot of MOLM-13 cells after transduction with shNT and shLAMP5-2.

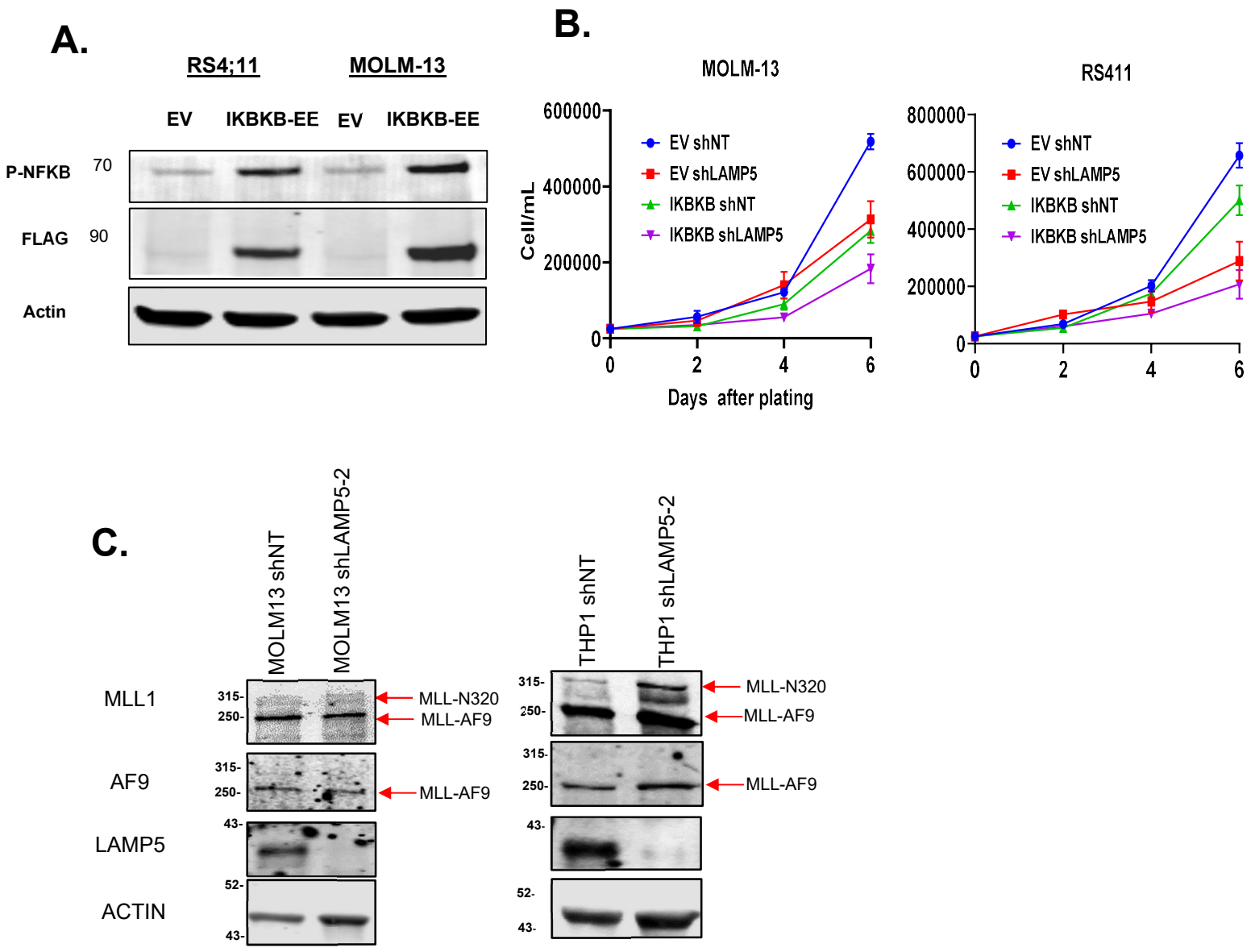

Supplemental Figure 5: (A) Western blot analysis showing overexpression of IKKB-EE (FLAG) and activation of p-NFKB. **(B)** In-vitro cell growth of MOLM-13 and RS4;11 overexpressing EV or IKBKB-EE upon LAMP5 downregulation. Data is from 3 technical replicates, representative of at least 3 experiments. **(C)** Western blot analysis showing the expression of the Germline MLL1 and MLL-AF9, C-term AF9, LAMP5 and actin after LAMP5 knockdown in MOLM13 and THP1 cell lines.

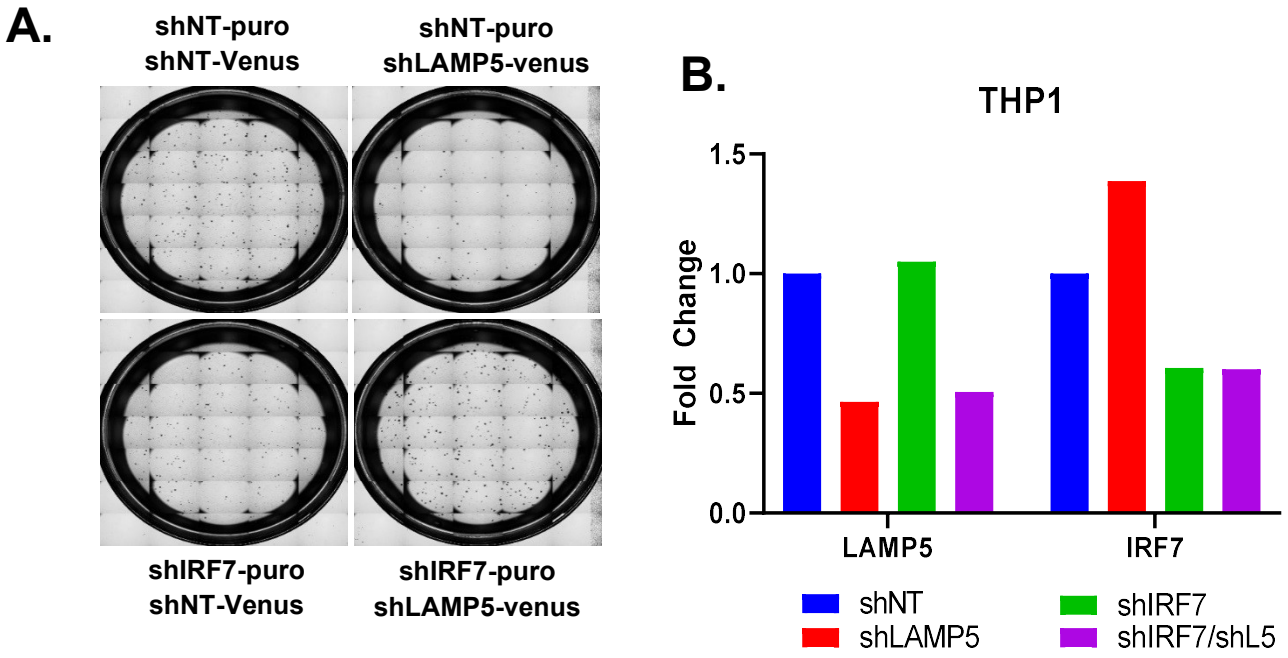

Supplemental Figure 6: (A) Representative images of THP-1 cells transduced with shNT/shIRF7/shLAMP5/shCombo(shIRF7/shLAMP5) after one week in methylcellulose. **(F)** Relative expression of *LAMP5* and *IRF7* after knockdown of LAMP-5, IRF7, or LAMP-5 and IRF7 together.

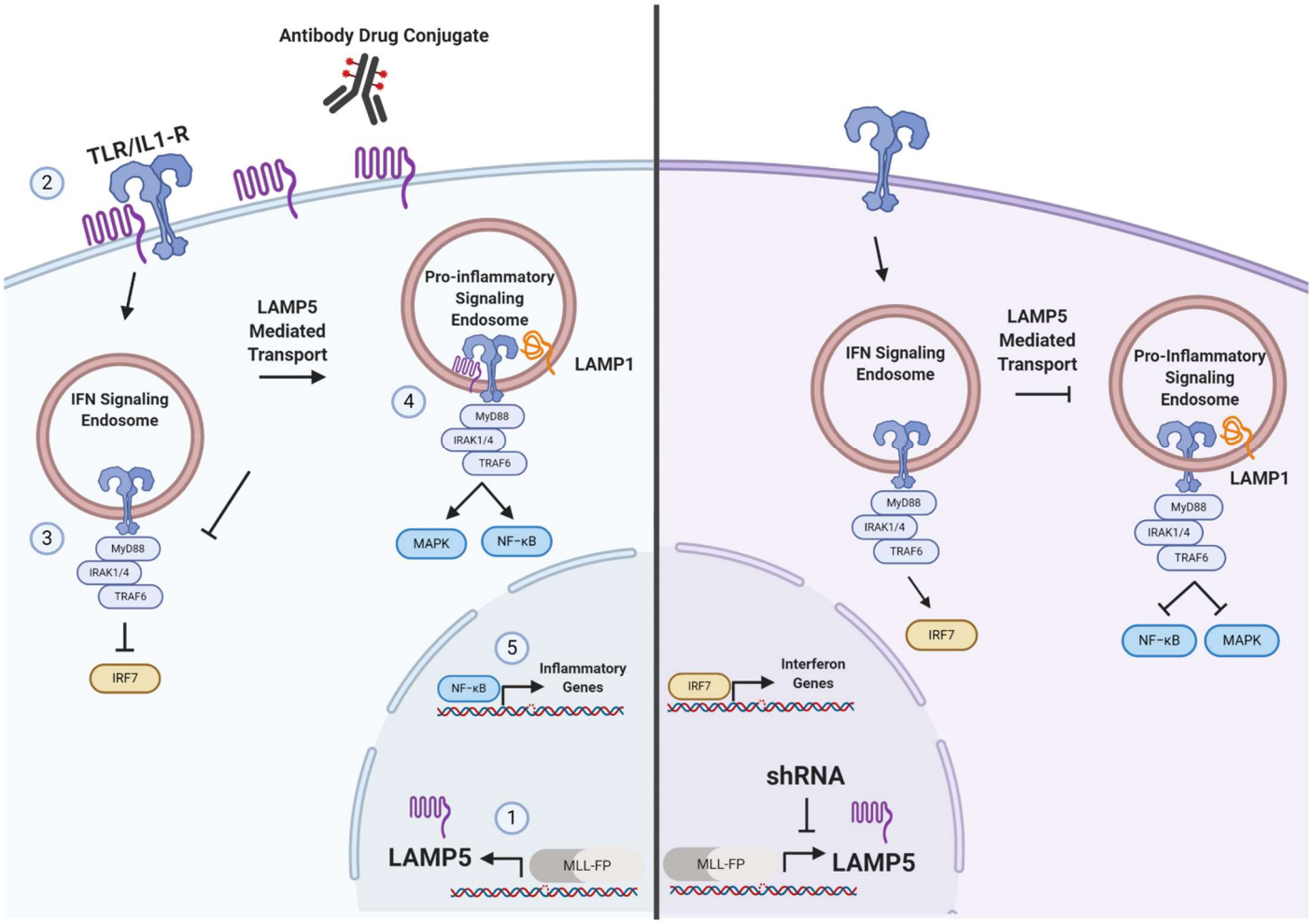

Supplemental Figure 7: Graphical Abstract. **Left panel:**.①The MLL-FP induces expression of LAMP5. ② LAMP5 gets internalized from the cell surface to the IFN signaling Endosome (IFN-SE), ③. ④LAMP5 is quickly shuttled to the LAMP1+ pro-inflammatory signaling endosome (PI-SE), activating NF-κB signaling. ⑤NF-κB activates pro-inflammatory signaling **Right panel:** Depletion of LAMP5 leads to blockage of transport and retention of TLR in the PI-SE, with activation of the IFN-SE and induction of Interferon related genes. Left panel depicts surface-LAMP5 can be targeted in MLL-r leukemias with immunotherapies.